REPORT NO. 1

ORIENTATION REPORT

TESTING METHODOLOGIES FOR FIBER OPTIC TRANSMISSION SYSTEMS

Prepared by
Bell-Northern Research Ltd.
Ottawa, Ontario

MARCH 1981

REPORT NO. 1

ORIENTATION REPORT

TESTING METHODOLOGIES FOR FIBER OPTIC TRANSMISSION SYSTEMS

FOR: DEPARTMENT OF COMMUNICATIONS
COMMUNICATIONS RESEARCH CENTER
P.O. BOX 11490, STATION H
SHIRLEY BAY
OTTAWA, ONTARIO K2H 8S2

DSS FILE REFERENCE: 13ST.36061-0-3309
DSS CONTRACT SERIAL: 1ST80-00116
BNR REFERENCE: P372/TR6734

PREPARED BY
BELL-NORTHERN RESEARCH LTD
P.O. BOX 3511, STATION C
OTTAWA, ONTARIO
K1Y 4H7

Government of Canada
Department of Communications

DOC CONTRACTOR REPORT DOC-CR-CS-81-014

DEPARTMENT OF COMMUNICATIONS - OTTAWA - CANADA

COMMUNICATION SYSTEMS RESEARCH AND DEVELOPMENT

TITLE: ORIENTATION REPORT - TESTING METHODOLOGIES FOR FIBER OPTIC TRANSMISSION SYSTEMS

AUTHOR(S): N/A

ISSUED BY CONTRACTOR AS REPORT NO: N/A

CONTRACTOR: BELL-NORTHERN RESEARCH LTD.

DEPARTMENT OF SUPPLY AND SERVICES CONTRACT NO: 1ST80-00116

DOC SCIENTIFIC AUTHORITY: METIN B. AKGUN

CLASSIFICATION: UNCLASSIFIED

This report presents the views of the author(s). Publication of this report does not constitute DOC approval of the report's findings or conclusions. This report is available outside the Department by special arrangement.

DATE: MARCH 1981

SUMMARY

The objective of the present contract is to define TEST METHODS for fiber optic transmission systems. This "Orientation Report" concludes the first phase of the contract by presenting:

1) the state of the art in characterization, modelling and testing of fiber optic components and systems, and

2) the major features of the approach to be followed by BNR.

The review indicates:

1) the importance of excitation and launching conditions on the characterization of fiber components (source, fiber, joint) and systems,

2) the interdependence of present characterization and testing methods for source, fiber and joint,

3) the emphasis of present testing methods on obtaining a steady-state characterization,

4) the lack of transient characterization (i.e. magnitude and length), and

5) the general incompleteness of current models and/or the incompatibility between them.

The approach to be followed by BNR will consist of:

1) the development of a theoretical model for all fiber components that takes into account their modal properties in a complete and compatible fashion, and

2) the definition of test methods using the theoretical model as a research tool to investigate, simulate and compare various test methods.

This theoretical work will be paralleled and reinforced by an experimental program that will:

1) validate the models of fiber components and systems, and
2) implement and evaluate the simulated test methods.

The theoretical and experimental program will focus on the modal characteristics of fiber components in an attempt to isolate the characterizations of sources, fibers and joints. A matrix representation of this modal behaviour using a WKBJ approach, (i.e. quasi-ray theory) will be the basis of BNR's forthcoming research.

No changes in the content or schedule of the contract work are foreseen at the present time.

TABLE OF CONTENTS

LIST OF FIGURES

LIST OF TABLES

NOMENCLATURE

BPO :	British Post Office (now British Telecom)
BTL :	Bell Telephone Laboratories
CWG :	Corning Glass Works
DMA :	Differential Mode Attenuation
DMD :	Differential Mode Delay
EMD :	Equilibrium Mode Distribution
EMS :	Equilibrium Mode Simulator
EMV :	Effective Mode Volume
FFP :	Far-Field Pattern
FWHM:	Full Width at Half Maximum
ILD :	Injection Laser Diode
LED :	Light Emitting Diode
LNA :	Launch Numerical Aperture
MPD :	Modal Power Distribution
NA :	Numerical Aperture
NFP :	Near-Field Pattern
NTT :	Nippon Telegraph Telephone
RMS :	Root Mean Square
WKBJ:	Wentzel - Krammers - Brillouin - Jeffreys

1. INTRODUCTION

The routine implementation of fiber optic systems is currently hampered by design, operational and maintenance problems. To ensure routine implementation a more certain characterization of fiber links is required. Characterization is the process by which the behaviour of a fiber link or of its components is determined from a transmission point of view. This may be done exclusively through experimental testing or else theoretically with a model. The model may be analytical or empirical. In both cases experimental data is generally required by the model. When the characterization process is complete and accurate, it is equivalent to a prediction process in that the gap between the specifications of a transmission system and its actual performance is narrowed.

Research organizations throughout the world have concentrated on characterizing, testing and modelling the various components of a fiber system with varying degrees of complexity and success. Very few organizations, however, have approached the problem with a global solution that allows:

1) a straightforward interconnection of the various submodels to produce an overall homogeneous model, and
2) a straightforward combination of the components' characteristics to evaluate the overall fiber link performance.

The objective of this contract is to define TEST METHODS that will lead to better system characterization. This will result in:

- efficient and economical system design through reduced overdesign, and
- improved performance monitoring and system maintenance through more meaningful testing.

To achieve this objective a model needs to be developed to simulate various test methods and to assess their suitability for fiber optic communication systems.

The test methods that will be defined may become standards in the field of fiber optics communications, giving Canadian manufacturers an edge over their foreign counterparts.

1.1 Objective of Report

BNR's proposed approach to the problem focuses on the modal behaviour of each optical element. This is the fundamental propagation mechanism in optical fibers. By keeping track of the evolution of the modes or significant mode groups along the optical link, the end-to-end response can be calculated.

This report compares the current characterization methods with BNR's approach. This comparison is made to determine the extent to which current testing and modelling methods will be incorporated in to the approach.

1.2 Outline of Report

Section 2 of this "Orientation Report" presents the conclusions of the first activity of the contract. It defines the major features of subsequent activities.

Sections 3 to 6 review the state of the art in the characterization of fiber optic components and fiber links. Current testing methods are presented first. Then modelling methods are reviewed. The respective merits and difficulties of these testing and modelling methods are discussed.

Specifically, Section 3 deals with launching conditions and the modelling of optical sources, as fiber and joint characterization depends on the excitation conditions. Section 4 discusses the attenuation and dispersion of optical fibers. Section 5 reviews the loss and mode mixing properties of joints (splices and connectors). Section 6 addresses the question of length dependency of link attenuation and dispersion.

Section 7 discusses the relative complexity and accuracy of the above methods of characterization, testing and modelling. In particular it compares them to the global approach chosen by BNR. It also determines to what extent they will be incorporated in BNR's approach.

Because of the very nature of the current characterization techniques and the intricate interplay of the components' behaviour, Sections 3 to 6 are somewhat interrelated. They overlap to the extent that:

- the fiber performance depends on the source excitation,
- the joint performance depends on the source and the incoming and outgoing fibers, and
- the link performance cannot be dissociated from the joint behaviour.

This report fulfils milestone 1 of the contract as per the work proposal.

2. CONCLUSIONS

This "Orientation Report" presents a review of current testing and modelling techniques for fiber optic components and systems. Following this review the work content of this contract remains essentially as laid out in the original work proposal although the detailed implementation has been more clearly defined.

The review emphasizes the need to relate the characterization of fiber components and systems to the exciting modal power distribution. Therefore, a model of MODAL behaviour of fiber components will be developed. This model will be used as a TOOL to research and simulate various testing methods.

The interest of the model will be in its homogeneous treatment of all fiber components from a MODAL point of view. This will allow for the characterization of the steady-state as well as the transient performance of fiber systems.

The model will have a theoretical and an experimental basis. The experiments will initially serve to validate the model and to determine numerical data for the model. Later, experiments will be used as a test bed for various testing methods according to the conclusions of the simulated test conditions.

The model will accomodate graded index fibers of arbitrary profile since the fiber bandwidth depends greatly on the actual profile. The model will use the WKBJ quasi-ray theory of Section 4.4.1 to account for the modal delay of fibers of arbitrary profile. An extension to arbitrary profile of the WKBJ approach of Section 5.5.1 will be used to represent mode mixing at joints. Modal attenuation will be modelled according to section 4.2.2 with the aid of experimental data. The experimental program will also measure the modal attenuation and delay of the fibers, and the mode mixing in fibers and at the joints. Spectral delay and attenuation will also be incorporated. Work will be required to establish a theoretical link between modal power distribution and measurable characteristics like near- or far-field patterns.

No changes in the content or schedule of the contract work are anticipated at the present time.

3. SOURCE AND EXCITATION CONDITIONS CHARACTERIZATION

Current testing methods for fiber and joint characterization control in some fashion the modal power distribution injected into the first fiber. The intent is to produce excitation conditions that yield a measurement independent of the source and length. This is known as a steady-state excitation.

Steady-state measurements began after it was recognized that measurements, in particular fiber attenuation, varied widely from manufacturer to manufacturer and from laboratory to laboratory when different sources and launch conditions were used.

Four methods are used to improve the consistency of measurements: 1) mode scramblers are used to randomize the power amongst all the guided modes, 2) mode strippers are used to remove the higher order and leaky modes so they do not perturbe the measurements, 3) the launch spot size and numerical aperture (NA) of the launch beam are restriced so as to excite only a subset of the modes the fiber can normally support, and 4) an extension of method (3) controls the launch beam to excite a given effective mode volume.

These four methods of controlling the launch condition are reviewed hereafter in Section 3.1. Means of characterizing the launching conditions or the source are reviewed later in Section 3.2.

3.1 Launch Methods

This section examines various launch methods used in an attempt to obtain consistent attenuation and dispersion results. It appears that attempts to obtain consistent measurement results were not reported until 1976.

3.1.1 Mode Scrambler

In 1976 the use of a compact device to attempt to achieve a steady state mode distribution was reported [1]. It consists of an etched fiber and a

normal one slightly spaced within a connector and held together with a higher index transparent adhesive (see Figure 3.1). The etching exposed the layer structure of the fiber and contributed to the randomization of the input light. Insertion loss with an injection laser was 0.5 dB, and its output far-field pattern (FFP) was reasonably independent of laser offset. Moreover, an offset of a core radius between this mode exciter and the test fiber could be tolerated to give 'steady state' consistent FFP and baseband frequency response measurements.

The above equilibrium mode simulator (EMS) launching device was used in a concatenated chain of spliced graded-index fibers [2]. Also, a mode scrambler [3] was used after each splice; this allowed accurate prediction of the total transfer function based on measurements for each segment, and it also increased total bandwidth over the situation without scramblers. Figure 3.2 shows a schematic of the scrambler, which consists of a fiber surrounded by a few larger diameter wires all within a heat-shrinkable tube; insertion loss was about 0.3 dB. In another study [4], splice loss increased with

Figure 3.1
Etched Fiber Mode Scrambler

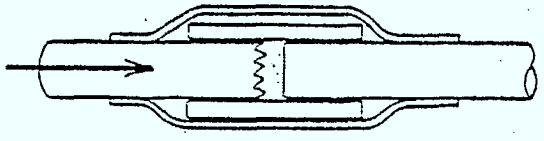

launch NA (LNA) to a saturation value when only a 3 m fiber length preceeded the splice, but the mode-filtering action of about 1/2 km of fiber virtually eliminated the effect. The tendency of the splice to expand the NA of the beam was also reduced by this filtering. An output mode filter reduced the output NA and increased splice loss by about 0.5 dB. These observations point to the desirability of an 'equilibrium NA' excitation for such measurements.

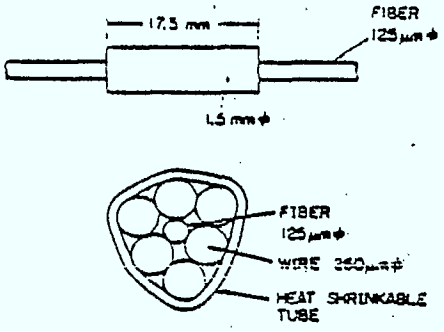

Figure 3.2
Tube and Wire Microbend Scrambler

Other short launching fibers have recently been used. A laser beam was launched via a lens into a step-index fiber with an NA slightly larger than that of the fiber to be measured [5,6]. The idea here is to provide a nearly uniform mode exciter. A transverse launch offset of up to 1/3 the core diameter produced little change in the FFP or the baseband response. Another version used a launch fiber (length and profile unspecified) with an adjustable bend (loss $<$ 1 dB) and launch NA (about half the fiber NA) so as to create a FFP to closely match that of the test fiber [7]. It was found that the FFP width (measured at 85% of the critical angle) had to be held within 3% in order that 0.05 dB reproducibility in connection measurements be maintained.

In another manifestation, three 1 m lengths of step, graded and step index fibers, respectively, are fusion-spliced together [8]. The step index fibers are to smooth and circularize the launch beam while the graded fibers are to provide angular mixing; this was checked by FFP observations. A GaAs injection laser diode was used and the scrambler loss compared to direct coupling to a fiber was about 1.5 dB. Bandwidth measurements were made as the source radial position was varied; with the scrambler and between

scramblers. Bandwidth variations of only a few percent were noted even in fibers that varied by an order of magnitude with source position without the scrambler. Similarly, with the scrambler pigtailed to the diode, a 25 μm lateral misalignment of the scrambler relative to the test fiber had negligible effect.

The use of a mode-filtering 'dummy fiber' has been systematically studied [9,6] to obtain equilibrium attenuation measurements. An LED with a 4 m pigtail was fusion spliced to the test fiber; the cutback length of the test fiber was also varied. Figure 3.3 shows 'excess loss' vs. dummy length with cutback length as a parameter. It was concluded that a 1/2 km dummy and a 2 m cutback are sufficient to come within 0.05 dB of the zero excess loss as referenced to a 10 m cutback. Jointed fiber measurements yielded consistent results. However, it is not clear whether an even longer cutback length would not have yielded a lower reference level. Also, the method is not applicable to bandwidth measurements because of the large distortion contribution of the dummy fiber.

The effect of bends on the FFP was studied in 1976 [10]. A step-index NA = 0.18 fiber wound around a 10 cm diameter drum was used; 100 turns were as effective as 500 in establishing an equilibrium mode distribution (EMD), but smaller radii with fewer turns were not studied. Tighter diameter bends were later used in a configuration [11] consisting of 4 to 6 pegs of about 1 cm diameter and about 1.4 cm center separation as in Figure 3.4. The FFP's exiting this scrambler and exiting a km of similar fiber compared well in width. In a frequency rolloff measurement, the baseband attenuations of two fibers summed closely when the scrambler was used.

3.1.2 Mode Stripper

Several 'mode strippers' were compared in a study [12,13] involving selective mode excitation and calorimetric loss measurement: fiber laid onto black felt with index fluid, with and without pressure, irregular 1 to 25 cm radius S-channel plus fluid, a double-S 2.5 cm bend radius plus fluid, and finally a grating mode scrambler. In all cases the fiber in the stripper was uncoated and the fluid had an index n = 1.47. Only the S-type devices gave an

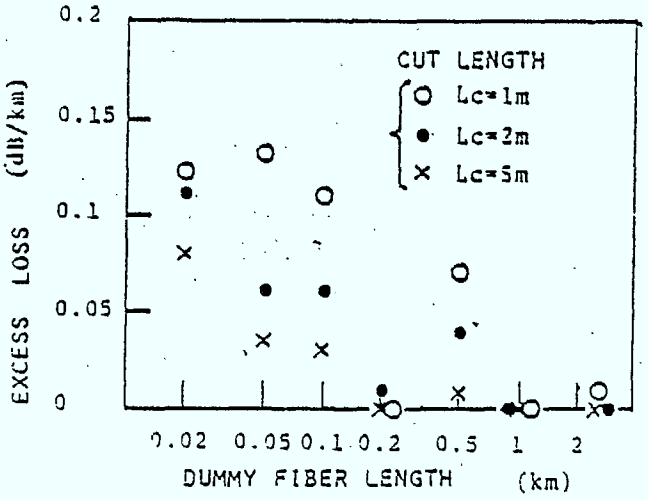

Figure 3.3
Dependence of Measured Fiber Attenuation on Dummy Fiber Length and Cutback Length

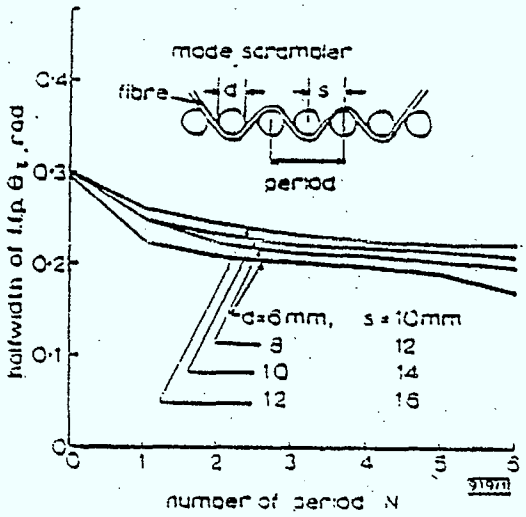

Figure 3.4
Peg-type Bending Mode Mixer: Effect of Configuration on Far-Field Pattern Width

attenuation reasonably independent of incident spot position when a short fiber length was used, with the regular bend version of Figure 3.5 being best in this regard. After 100 m from the launch end, attenuations with or without the regular S were the same, confirming the natural filtering action of the fiber.

Figure 3.5
S-Shaped Mode Stripper

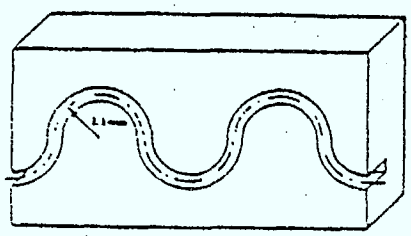

It was found that [14], with the S-filter applied to a 2.2 km fiber, increasing the launch NA from 0.15 to 0.25 increased attenuation by 0.2 to 0.4 dB/km over a spectral range of 0.8 to 1.3 μm. However, 5 turns of the fiber around a 1/2" diameter mandrel gave NA-independent results (about 0.2 dB/km lower than the S-filter with the 0.15 NA) coinciding well with a 1.2 km dummy launch fiber measurement. The FFP's also agreed well. Further work [14] determined that the mandrel wrap gave an attenuation at 0.82 μm that was 0.2 dB/km lower than the irregular S and 0.3 dB/km lower than the 2.5 cm radius S. Sharper bends filter out lossy higher order modes and if the fiber coating is of an index lower than that of the cladding, a cladding mode stripper may be necessary. More detailed instructions [14] require that the mandrel be smooth, that the turns be taped on with minimum tension covering a maximum of 1/2" along the mandrel, that there be no other sharp fiber bends and that there be at least a 2 m cutoff with at least 1 m after the mandrel.

Further experimentation fine-tuned the mandrel wrap mode filter [15]. Fibers at Bell Telephone Laboratories (BTL) were overfilled and the far-field pattern widths Θ_2 noted for the full length. The mode filter was then applied to the short length and width Θ_1 noted. The plot of Figure 3.6 gives the change in widths vs diameter of the mandrel when 5 turns are applied around it; just under 7/8 in. appears best. Similar plots could be generated for fewer turns, or for fixed diameter and a variable number of turns. Clearly, these parameters will change with fiber design (core/cladding of 55/110 μm, NA of 0.22 here). With a 5-turn 1/2 in. mandrel, the attenuations of 5 lengths of 1 km each were measured. The sum of these was about 1 dB below that of the 22 dB concatenated loss. Splice losses reduce the discrepancy to 0.5 dB or 0.1 dB/km.

The use of microbends induces mode mixing that can hasten the approach to an equilibrium mode distribution (EMD). Sandwiching the fiber between two gratings or between sheets of abrasive paper [16] and adjusting the pressure to give 2-3 dB loss tends to overfill higher order modes. To give consistent attenuation or distortion measurements on concatenated fibers, it was found that slight underfilling of the NA was required. Another microbend scrambler

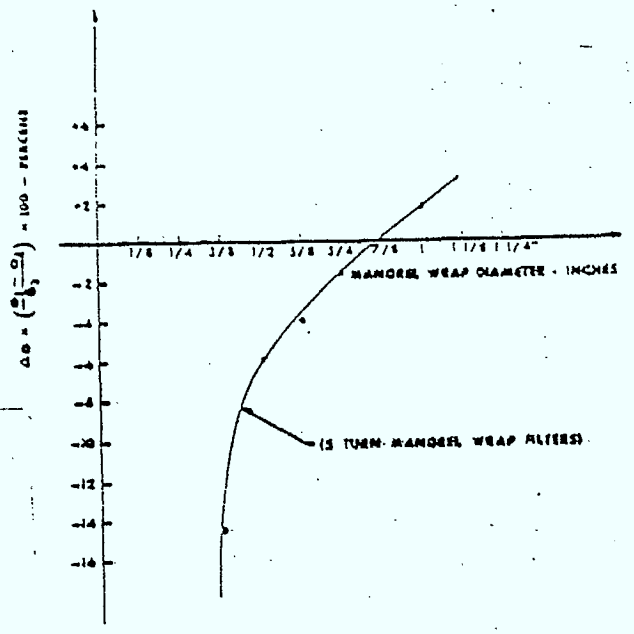

Figure 3.6
Change of Far-Field Pattern Width With Diameter of 5-Turn Mandrel Wrap When Comparing the Filter Output With the Long Fiber Output

[17] consisted of steel balls of 1 to 5 mm diameter randomly distributed over the surface of a bed in such a way that the tops of all balls were at the same level. About 1 m of fiber was subjected to an adjustable pressure plate; this was followed by a mode stripper (if the fiber coating did not itself act as a mode stripper) of 0.5 m fiber within immersion oil. Pressure was adjusted and the FFP observed such that the ratio of the angles at 50% and 5% intensity fell between 0.5 and 0.7 for graded-index fiber. For jointed cables up to 8 km in length, attenuations agreed to within 0.2 dB/km. Pulse broadening added slightly sub-linearly.

3.1.3 Restricted Launch Conditions

It was recognized in 1976 [18] that, even with mode scramblers or strippers, some (leaky and radiative) lossy modes were generally launched into graded index fibers. For full core excitation, even a relatively small 0.1 launch NA (LNA) overestimated by 1.2 dB/km the long length 'steady-state' loss. In a step-index fiber this launch underestimated by 0.2 dB/km the steady state 4.3 dB/km value; this is expected since in such a fiber severely lossy modes are excited only when the meridional NA is exceeded.

The method of restricted beam launch has been proposed by several countries [19] to give good linearity of attenuation with length. Specifically, a launch spot diameter 50% of the core diameter and a launch NA 60% of the

short-length fiber NA were recommended [20]; pattern widths were to be measured at the 10% intensity points. Later, several laboratories [21] compared attenuations measured with various combinations of launch conditions, microbend scramblers, strippers, and S-grooves. In some cases, comparisons of the cutback and backscattering methods were made. Fiber cores ranged from 30 to 63 μm and NA's from 0.15 to 0.46. Results were not totally conclusive, but it appeared that small spot (40 μm) small NA (0.12) launch ensured the best repeatability. An additional form factor [22], the ratio of 50% to 5% intensity widths in the far-field has been used to more accurately match far-field distributions.

Mode limitation can be accomplished at the output, rather than the input, end [25]. Here launch overfill is used while mode filtration at the detector is accomplished via a circular aperture stop placed in the image of the fiber's output near-field.

3.1.4 Effective Mode Volume

Recently, an interesting consolidation of varying limited launch and jointing conditions has been proposed by Corning Glass Works (CGW) [24,25]. This approach defines an 'effective mode volume'

$$EMV = (D \sin\Theta)^2 \qquad (3.1)$$

where D is the full-width at half maximum (FWHM) of the near-field and Θ is the half-width at half-maximum of the far-field. (Best correlation was claimed for the width at half maximum as opposed to the width at 5 or 10% intensity.) One rationale for the EMV is that for a uniform Lambertian source it is roughly proportional to the optical power; moreover, it is proportional to the number of modes in a parabolic guide. It is believed (there is a controversy on this) that rapid mode mixing occurs within a mode group (corresponding to a particular value of radius and angle), so that different combinations of D, Θ yielding the same EMV also have identical attenuation rates.

3.2 Models of Excitation Conditions

Characterizing and modelling the optical source consists essentially in determining how the optical power is launched into the fiber and distributed amongst the fiber modes. To some extent the matter is similar to joint characterization, especially if the end of the fiber pigtail is considered to be the system source.

Because of the reciprocity theorem of Helmoltz it can be considered that if a relationship exists between the modal power distribution of a fiber and its near-field and far-field pattern (NFP and FFP), a source with the same NFP and FFP excites the same modal power distribution in the fiber.

3.2.1 Near Field Pattern and Modal Power Distribution

A number of authors addressed the problem of relating the modal power distribution (MPD) to the NFP or FFP. For fibers of arbitrary profile, Leminger and Grau used the WKB formalism of geometrical optics [26]. They concluded that a unique relationship between the MPD and the NFP does not exist unless the MPD is a function of the propagation constant β only or a function of the momentum mode number ν only.

Piazzola and de Marchis had determined earlier that the MPD is a function of the spatial derivative of the NFP for α-profile fibers when the MPD depends on β only and is uniformly distributed within a degenerate mode group [27] (see also [28]).

Daido reached a similar conclusion using the concept of provisional cladding [29]. He also discussed the property of fibers to distribute the power uniformly within a degenerate mode group.

3.2.2 Far Field Pattern and Modal Power Distribution

For fibers of arbitrary profile, Leminger and Grau [26] concluded that the relationship between the MPD and the FFP is not unique and has no analytical solution even when the MPD is a function of β only or of ν only.

For α-profile fibers the MPD can be determined via elaborate expressions that contain the FFP and its first or second derivatives.

It is also presumed - but not proven - that the simultaneous use of the FFP and NFP does not help to determine the MPD of a fiber of arbitrary index profile [26]. This presumption needs to be validated.

Daido et al computed the FFP corresponding to an arbitrary power distribution [30]. Then they outlined a recursive method to compute the MPD from the NFP in the case of an α-profile.

3.3 Discussion

The control of launching conditions aims at reducing the dependence of fiber and joint characteristics from the source, and at improving their linearity with length.

Since the power launched by the actual source of an operational system is not likely to duplicate the controlled launching conditions of the test equipment, the operational system will exhibit a transient behaviour before reaching its steady-state behaviour. In some cases the steady-state may not be attained before a joint creates another transient. The magnitude and the duration of the transient are important to the characterization of the overall system performance. With present sources, the use of a launch controller in an operating system may introduce an excessive loss into the system.

To characterize the power actually launched into the fiber in a manner compatible with its modal description, modal power distributions can be found from near-and far-field patterns under certain conditions. Extension of this concept to fibers of arbitrary profile will be investigated since actual fibers do not always have an α-profile.

This work is expected to enable us to simulate various launch conditions and devices and provide the data base to permit an optimum selection.

4. FIBER CHARACTERIZATION

4.1 Fiber Parameters

Traditionally the attenuation and the dispersion of a transmission medium have determined the performance and the reach of a transmission system. This remains true with optical fibers. However, the attenuation and the dispersion of a fiber are now recognized as highly dependent upon the testing methodology and the peculiarities of the actual test set-up. This is because optical fibers as well as splices and connectors attenuate and delay various modes to various degrees. Historically, the concept of differential mode delay (DMD) has existed (perhaps not with that terminology) as long as that of multimode dispersion. Differential mode attenuation (DMA) was not formalized prior to 1971, while mode mixing was recognized in 1972. The effects of these phenomena upon measured attenuation and dispersion were subsequently studied, initially in single and later in concatenated fibers.

The performance of fiber systems depends in some complex fashion upon some detailed fiber parameters like the core diameter, the numerical aperture (NA) and the refractive index profile. Testing methods to determine these fiber characteristics are not discussed in this document as the user is not likely to perform the corresponding measurements to determine the attenuation and dispersion of his system.

4.2 Testing Methods for Fiber Attenuation

4.2.1 Spectral Attenuation

Fiber attenuation consists of two components. Absorption converts light into heat and is an intrinsic part of doped silicas at wavelengths exceeding 1.45 to 1.8 μm, depending upon the dopant. Impurity absorption due to transition metal ions has been largely eliminated in modern fibers, but the OH^- ion has several absorption peaks with the major one around 1.38 μm. Additional absorption can occur due to nuclear radiation. Absoption measurements can be made by microcalorimetric means.

Scattering is the other component of attenuation. It refers to light escaping the propagation direction, either out of the fiber or into the trapped backward direction. It is due primarily to material Rayleigh index fluctuations and possibly some structural imperfections. Scattering attenuation increases as the inverse fourth power of wavelength toward shorter wavelengths. High optical powers within the fiber can also induce non-linear scattering effects. Ordinary scattering is usually measured with a cube detector or else an integrating sphere surrounding some signficant length of fiber.

The difficulty of separately measuring absorption and scattering has restricted its use to only a few fiber manufacturers. From a user viewpoint, only the total attenuation is measured, either at discrete wavelengths of interest (typically 0.85 and 1.3 μm using light-emitting diodes) or across a spectrum extending from about 0.7 to 1.7 μm (usually utilizing an incandescent white light source and a monochromator, with a spectral linewidth not exceeding about 10 nm).

4.2.2 Differential Mode Attenuation

As discussed in Section 3, attenuation is sensitive to launch conditions. The best method of probing this is by exciting specific modes [31] or mode groups [32,33] within a fiber and measuring their attenuation over some fiber length. The latter is easier to implement; a light cone with a small spot size and small NA (both properties can be simultaneously attained to only a limited extent) incident upon the fiber face will excite only a small number of modes. Usually only non-azimuthal modes are excited since normal incidence is used. The mode group number is then proportional to the radial coordinate of incidence squared. With recent fibers, the attenuation is virtually uniform for all but the highest order mode groups near cutoff.

4.2.3 Cutback Method

This is the earliest method of measuring optical fibers, and although not the most convenient, it is still recognized as being the most accurate. The source, with specified launch conditions, is coupled to the full fiber (link)

length and the output power is measured. Without disturbance of the input end, the fiber is cut to within 1-2 m of the launch point and the output power is again measured. In the field this usually requires separate detectors (and persons) at the long and short ends. The power ratio (or logarithmic difference) yields the loss. Two power measurements per fiber specimen are required.

4.2.4 Insertion Loss Method

The short length measurement is performed as above on a fiber sample similar to the specimens being evaluated. The output power serves as the reference. The full length specimen is then jointed onto the sample fiber and the output power measured. Note that the joint loss is included, and an approximate correction must be assumed. The full length measurement is repeated for each specimen in turn, with an attempt to make the joints reproducibly. After the reference calibration, one measurement per specimen is required. Joint loss measurements are discussed in Section 5.3.

4.2.5 Backscatter Method

An optical time domain reflectometry (OTDR) response for the specimen is displayed, preferably logarithmically [34]. The backscattered power levels at the time scales corresponding to sections near the input (just after any initial backreflection) and near the output (just before any final backreflection or end of backscatter) are noted. The power ratio (or logarithmic difference) is taken to be twice the loss; equal backscattering levels at the input and output ends are implicity assumed. Alternatively, the logarithmic slope at a point on the OTDR trace is taken to be twice the attenuation rate at the corresponding fiber location, if the backscattering is constant along that section. One near-end measurement per specimen is required.

4.3 Testing Methods for Fiber Dispersion

Fiber dispersion may be divided into chromatic and multimode components. The information carrying capacity is limited by pulse spreading in the time domain,

or equivalently by amplitude rolloff and non-linear phase delay in the modulation frequency domain. Commonly, this is specified by an impulse response, its full-width at half-maximum (FWHM), its full root mean square width (typically in nsec), or else by a frequency response, or the 3 dB optical (6 dB electrical) bandwidth (typically in MHz). Values may be normalized to 1 km by some method (see Section 6.2).

4.3.1 Chromatic Dispersion

Chromatic Dispersion is due to the fact that different wavelengths from a source experience different delays and attenuations. Hence, within a fiber length L a source of spectral width $\Delta\lambda$ centered about a wavelength λ will give rise to a temporal spreading [35]

$$\Delta T(\lambda) = \frac{d\tau}{d\lambda} L\Delta\lambda + \frac{1}{2} \frac{d^2\lambda}{d\lambda^2} L(\Delta\lambda)^2 \qquad (4.1)$$

Here $\tau(\lambda) = N(\lambda)/c$ is the mode-averaged group delay per unit length; $N(\lambda)$ is the group index related to the phase index $n(\lambda)$ by the relation

$$N(\lambda) = n(\lambda) - \lambda \frac{dn}{d\lambda} \qquad (4.2)$$

Usually, only the first term of Equation (4.1) is used, but near a wavelength λ_o where it vanishes, the second derivative must be used. This is especially true with LED's of broad spectral width $\Delta\lambda$ [36]. Moreover, even with a monochromatic source, the modulation frequencies themselves may contribute to dispersive effects [37], but this is of concern only in high bandwidth monomode fibers.

4.3.2 Spectral Group Delay

The most direct way of obtaining chomatic dispersion is to measure the group delay per unit length $\tau(\lambda)$ as a function of wavelength, and to use Equation

(4.1). This requires a large number of pulsed sources. A particularly attractive multiwavelength laser is a fiber Raman laser. A co-operative Bell-Northern Research/Communications Research Centre effort utilized the apparatus of Figure 4.1 to produce the group delay curve of Figure 4.2. Note that the group delay has a minimum value occuring at the optimum wavelength $\lambda_o = 1.304\mu m$ at which the first-order chromatic dispersion derivative is zero.

Another way of obtaining the group delay is to use Equation (4.2) after obtaining the refractive index $n(\lambda)$. Such classical optical measurement are usually performed on a prism glass sample [38] but the material so analysed may not correspond to the fiber material. A recent autocorrelation technique [39] looks promising, but it may apply only to monomode fibers. Finally, chromatic dispersion may be obtained approximately by measuring fiber pulse broadening utilizing two or more sources centred about a common wavelength, but possessing different spectral widths [40]. The overall pulse spreading T is given by

$$T^2(\lambda, \Delta\lambda) = \left(\frac{d\tau}{d\lambda} L \Delta\lambda\right)^2 + T_m^2(\lambda) \qquad (4.2)$$

where the multimode dispersion contribution (width T_m, see next paragraph) has been included. A plot of T vs $\Delta\lambda$ can be extrapolated to $\Delta\lambda = 0$ and the chromatic and multimode contributions at wavelength λ are separated.

4.3.3 Multimode Dispersion

Multimode Dispersion is due to the fact that different fiber modes experience different delays and attenuations. Furthermore, a profile dispersion occurs because the refractive indices of fiber glasses are functions of wavelength; hence an index profile optimized for minimum multimode dispersion at one wavelength will not be optimum at another wavelength. This is expressed by the $T_m(\lambda)$ variation in Equation (4.3).

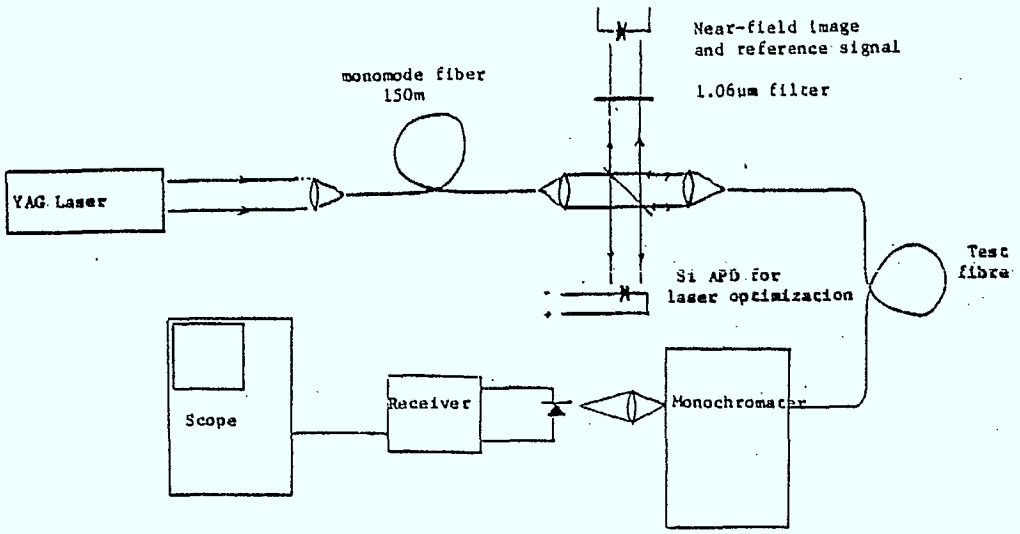

Figure 4.1: Schematic of a Raman Fiber Laser for Group Delay Measurement.

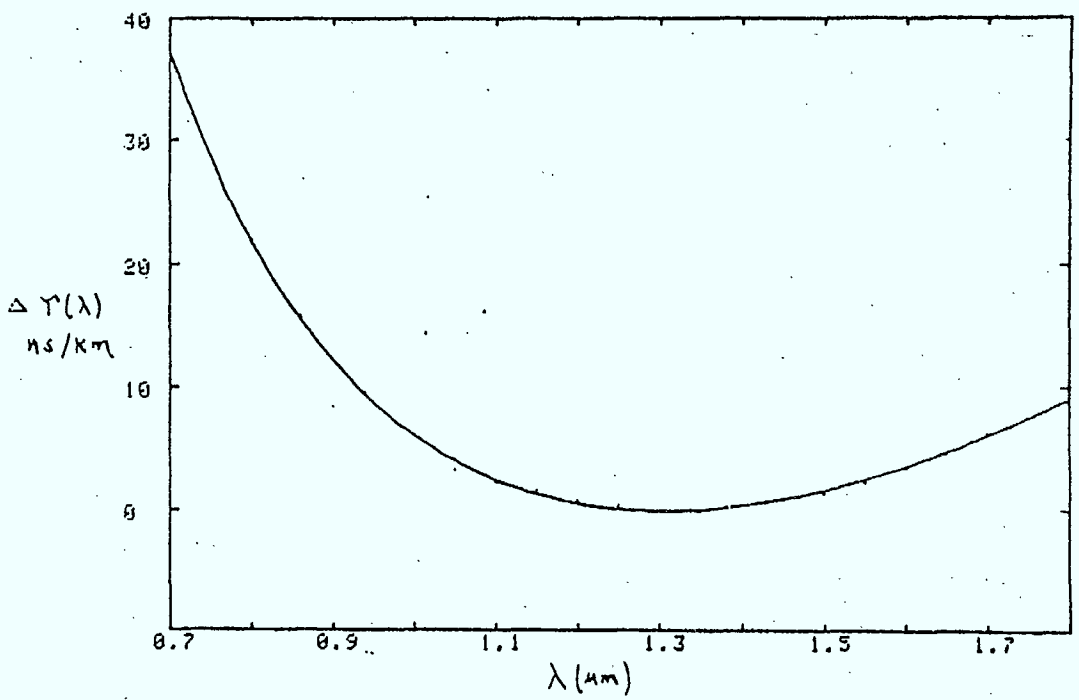

Figure 4.2: Spectral Group Delay Showing Measured Points and Best Fit Approximation. The Delay is Relative to its Minimum Value at the Optimum Wavelength λ_o where the Derivative (First-Order Chromatic Dispersion) is Zero.

4.3.4 Differential Mode Delay

Dispersion is even more sensitive than attenuation to launch conditions. For example [8], with spot excitations at 0, $\pm$ 0.5, $\pm$ 0.9 relative radial distances, the corresponding bandwidths for a multimode fiber were 450, 360 and 520 MHz respectively. Preliminary calculations at BNR concerning variable cone launches have shown similar type behaviour, including the non-monotonic behaviour with increasing mode group number. Experiments have shown [41] that the behaviour of delay vs radial excitation is quite erratic and depends upon wavelength, as in Figure 4.3. The technique is recognized as being the optimum method for profile optimization and multimode dispersion minimization. As discussed later in Section 6.2.2, the technique has been recently applied to jointed fibers.

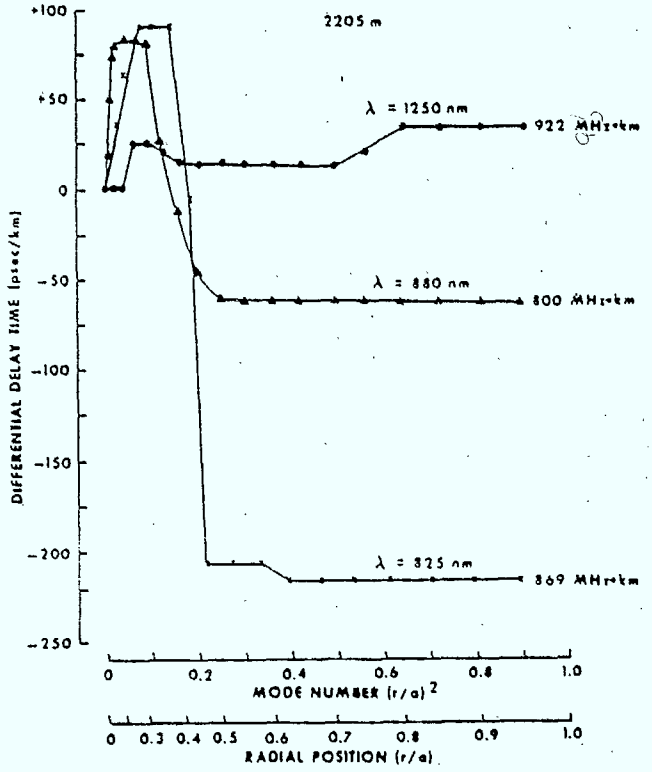

Figure 4.3: Differential Group Delay Time Versus Radial Position as a Function of Wavelength

4.3.5 Mode Mixing

Mode mixing or mode coupling tends to average out intermodal delay differences. This results in multimode dispersion along a homogeneous fiber increasing sublinearly with length. However, with the lowest loss fibers this effect is not very strong. At joints however, particularly between mismatched fibers, localized mode mixing occurs. This can accentuate the equalization effect occuring when low modes are coupled into high modes and vice versa. A second effect of both distributed and localized mode mixing is to increase the loss because of the unavoidable scattering of some modes into the unbound domain.

Measurements of mode mixing parameters are not very reliable, particularly since the parameters vary amongst modes, and modal power distributions are difficult to measure.

4.3.6 Dispersion Measurement

In its most elegant form, fiber dispersion is specified in terms of an impulse response h(t) defined via the convolution

$$r(t) = \int_{-\infty}^{\infty} h(x)s(t-x)\,dx, \tag{4.4}$$

or by its (complex) baseband frequency response H(f) defined by the product

$$R(f) = H(f)S(f). \tag{4.5}$$

Here [h(t), H(f)] are Fourier transform pairs as are the input signals [s(t), S(f)] and the ouput signals [r(t), R(f)].

Sometimes a simpler description is used. For example, from Equation (4.4) the root mean square widths W satisfy

$$W^2(h) = W^2(r) - W^2(s). \tag{4.6}$$

This is sometimes applied to the FWHM (a Gaussian approximation). An equivalent approximation in terms of the 3 dB widths F is:

$$F^{-2}(H) = F^{-2}(R) - F^{-2}(S).$$

Both chromatic and multimode dispersions are included in these time and frequency domain measurements.

a) Time Domain Measurement

The cutback technique is used, with the short length pulse being the source-detector input. An input pulse no wider than about half the output pulse should be used for sufficient accuracy and power levels should be made comparable to avoid detector nonlinearities. Repetitive pulses with phase-lock detection or signal averaging may be used over long spans. Laser chirping, in which faster moving longer wavelengths are emitted earlier in the pulse, should be avoided. Either the approximate width formula of Equation (4.6) is used, or else numerical deconvolution. In the latter approach the pulses are transformed into the frequency domain and by Equation (4.5) H(f) may be solved for. Usually, only the magnitude rolloff is obtained, but the phase cannot always be ignored. The 3 dB bandwidth may be read from the curve. Inverse Fourier transformation to the time domain yields the impulse response h(t). Computer software is sometimes a problem with respect to signal to noise ratio and data quantization.

b) Frequency Domain Measurement

Here a swept modulation frequency of the form $(1 + m\sin 2\pi ft)$ is applied to the fiber. The reduction in the modulation depth m yields $|H(f)|$ while the sinusoidal shift yields phase. A spectrum analyzer yields only magnitude whereas more expensive equipment such as a network analyzer gives phase as well.

4.4 Fiber Models

4.4.1 Multimode Dispersion Models

a) Early Step Index

Historically, the dielectric rod waveguide was studied back in 1910, but the theory of the clad optical guide did not appear until 1961 [42,43]. Only what is now called the step-index guide - with a uniform core index n_1 and a uniform cladding index n_2 - was considered, in the infinite cladding approximation. As in all waveguide problems, the fields were assumed to vary harmonically in the time and axial coordinates, exp $i(\beta z-\omega t)$. Maxwell's field equations reduced to a scalar waveguide equation in terms of J-type Bessel functions in the core, and K-type modified Bessel functions in the cladding. The fields were sinusoidally periodic in the crossectional angular coordinate ϕ, and boundary conditions at the core/cladding interface led to a characteristic equation from which the propagation wavenumber β for all allowed modes could be derived. The Poynting vector allowed power distributions to be computed for the modes.

The ray-optics description of such a guide is exceedingly simple, at least to first order. For a particular ray the total internal reflection condition leads to simple angle preservation both with the axis and the surface normal in crossection. For small crossectional areas, ray quantization becomes important, and applying interference conditions in the z, ϕ directions later led to [44] a 'modal' characteristic equation. As expected for ray optics, this was the ray wavelength limit of the wave optic equation obtained previously. The ray optic approach suffers further from the fact that power distributions are not easily derived from it.

The wave-optic approach was further simplified [45-47] for the case of small core/cladding index differences, i.e. $\Delta = (n_1 - n_2)/n_1 \ll 1$. This approximation is justified for modern fibers with Δ's ranging from a few tenth's to a few

percent. Some of the exact (HE and EH) modes now combine into degenerate modes that are linearly polarized (LP) transverse to the propagation direction and somewhat simplified equations for the modal propagation wavenumbers ($v_p = \omega/\beta$ is the modal phase velocity) and power densities result.

When total internal reflection occurs off non-planar surfaces, tunnelling leaky modes can occur [48]. These modes correspond to non-meridional (skew) rays that can enter the fiber with an acceptance angle exceeding the meridional NA. This acceptance angle increases with increasing skewness. The corresponding attenuation also increases due to a tunnelling into the outer regions of the cladding. It was later realized [49] that such modes contribute to fiber length-dependent attenuation and dispersion effects.

b) Early Graded Index

In 1954 it was reported [50] that a cylindrically graded rod lens could be used to periodically refocus rays normally incident upon its entrance face. The index profile was of the form of a hyperbolic secant and was later treated by modal methods [51] and the WKB approximation [52]. This profile is exact for meridional rays, but helical rays require [52] a distribution of the form $n_o(1 + Ar^2)^{-\frac{1}{2}}$, since no single index distribution can image (or equalize the group velocities) of all rays. Both index distributions are quadratric to first order, and this can image all paraxial rays [53]. Corrective gas-lens guides were another inspiration for inhomogeneous focusing media, and an alternate form of the WKB approach was developed [54].

Another development was that of mode mixing [55] which had the potential of partially averaging out modal group delays and thereby reducing intermodal pulse spreading. This, along with index grading, provided an alternative to ultra-low dispersion monomode guides [56]. Theory now shifted away from the step index profile and below we classify the general routes it has taken. Only a small fraction of the hundreds of literature references are cited.

c) Ray Methods

The most straightforward way to begin utilizing the general ray equation is:

$$\frac{d}{ds}\left(n \frac{d\bar{r}}{ds}\right) = \text{grad } n \tag{4.6}$$

where $\bar{r}$ is the position of the ray path and s is the distance along it. The rate of change of the weighted tangent is in the direction of maximum increase of the index gradient. It is found [57-59] that for a particular ray of wavenumber kn(r) in a cylindrical medium, the axial wavenumber

$$\beta = kn(r)\cos\Theta(r) \tag{4.7}$$

(where $k = 2\pi/\lambda$, Θ is the axial angle) and

$$\nu = krn(r)\sin\Theta \sin\phi \tag{4.8}$$

(where ϕ is the azimuthal ray angle in the fiber crossection) are constants of the motion. The azimuthal component of the ray is ν/r. Phase and group delays may then be calculated [57-60] in terms of n(r) and the initial conditions at the input face.

The above suffers in that it is very difficult to specify the launch (initial) conditions for all rays. Moreover, ray power distributions are very difficult to obtain.

d) Modal Method

Here one attempts a solution of the waveguide equation at least to within the small index difference LP approximation. For parabolic index guides the primary field functions are Laguerre polynominals with unbounded core, and Whitaker/Kummer functions if a cladding is added [61]. Power-series solutions may also be attempted. The results are quite complex, not easily interpretable in terms of experimental parameters, and not applicable to more realistic imperfect power-law profiles. For this reason, a number of more approximate methods, as outlined below, have been developed.

e) WKBJ Method

The WKBJ method, named after Wentzel, Kramers, Brillouin and Jeffreys is the most commonly used approximate method and provides a bridge between the ray and wave approaches. There are basically two formalisms [54,52], both of which assume small index gradients over distances of a light wavelength. The first deals with a compound mode group number $m = 2\mu + \nu + 1$ where μ is the number of modal field nodes along a radius and ν is as in Equation (4.8); the second separates out μ, ν and quantizes the radial coordinate of the wavenumber (from Equations (4.7) and (4.8))

$$q(r) = [k^2 n^2(r) - \beta^2 - \nu^2/r^2]^{\frac{1}{2}}. \qquad (4.9)$$

Equation (4.9) indicates that the ray exists classically within the field oscillatory region (exp iqr) where q is real; outside of this region the fields are evanescent. Leaky modes are those for which β reduces such that beyond some distance into the cladding q is again real; tunnelling then occurs through the region extending from the outer part of the core into the inner part of the cladding and leads to variable excess loss.

The latter approach has been the most refined [62] and used [63], although it is not known which of the two is more accurate or if the two are equivalent [64]. In both WKBJ the modal fields and power distributions can be obtained [65,66] but usually only modal group delays are computed. This (and others below) suffers from not being able to readily insert input launch conditions, nor to account for differential mode attenuation, mode mixing, and chromatic and profile dispersions, although progress is being made in this direction [67].

f) Stratification Methods

These techniques first approximate the real refractive index into a stairlike approximation. Uniform index theory is applied within each region. The steps are made as small as allowed by the computing time. Originally this was applied to analyze diffusion at the core/cladding interface [68] and graded monomode

operation [69]. More recently it has been applied to practical profiles to obtain accurate values of both modal delays and power distributions [70]. The complicated numerical methods and long computational times have discouraged widespread use.

g) Perturbational and Variational Methods

Both of these begin with an 'exact' analytical solution to a known profile, such as the parabolic one. Neither of these [71,72] have gained widespread acceptance, perhaps because of numerical complexity and differences when compared with some known exact results [73,74].

h) Hamiltonian Method

This is essentially a ray-like approach recast in somewhat more elegant form. It has seen only limited use [75] and cannot treat power distributions.

i) Propagating Beam Method

As with most lightguide approximations, this method begins with the scalar Helmholtz equation for fields. This is transformed into a further approximate Fresnel equation which is then applied incrementally along the fiber axis. Fourier techniques play a prominent role, and rather involved window functions must be employed to avoid spurious resonance in results; certain launch conditions have similar effects. The numerical complexity may explain why the method has, over several years, not progressed beyond the originating authors [76]. Solutions can be computed only for a propagation distance of a few cm, and the claim is made that tunnelling modes virtually disappear within such distances. Another practically significant prediction is that modes with low azimuthal number are significantly affected by a profile central dip (in agreement with WKBJ). Both types of modes lead to pulse tails that can significantly extend RMS pulse values with only a small impact on 3-dB bandwidth.

j) Evanescent Field Method

Here the scalar fields are expanded, in both amplitude and phase, in terms of the reciprocal wavenumber (i.e. wavelength) [77,78]. The phase is allowed to be complex, corresponding to evanescent waves, and this avoids the problematic caustics of WKBJ theory. However, it appears to treat only polynominal profiles of a rather restricted nature, and hence may not be applicable to most measured profiles. Furthermore, it seems to require averaging procedures to dump out unstable oscillations in the numerical technique. Power profiles and variable launch conditions have not yet been attempted.

k) Maxwell Equation Method

Recently [79], a matrix formulation of Maxwells's equations has been applied to the cylindrical fiber geometry to derive 'exact' numerical solutions. Both power distribution and group delays are computed. Early results show that differences with the WKBJ method may be important for the design of very high bandwidth fibers.

4.4.2 Mode Mixing Models

All the above methods are concerned with predicting fiber properties given the refractive index profile and excitation conditions. Neglected, however, is the mode mixing phenomenom of Section 4.3.5 that can drastically affect the length dependence of transmission properties, particularly of dispersion in jointed fibers. Two theories have arisen to take this into account, giving little emphasis to exact index profiles and detailed group delays.

a) Coupled Mode Equations Method

The cross-sectionally integrated electromagnetic fields are taken to be coupled to each other via some imperfect perturbed index distribution [80]. With weak and random coupling, the field equations are transformed into a simpler form involving modal power. The power change vs distance for a particular mode includes loss due to attenuation and coupling into other modes; some gain occurs due to coupling from other modes. The equations may be cast into matrix form and solved perturbationally.

Two significant features result. First, the addition of continuous mode mixing gives multimode dispersion a sublinear increase with length, approaching the square root dependence for long lengths. Second, this improvement in bandwidth, purposeful or not, comes at the price of increased loss due to scattering of high order modes into unbound modes.

b) Diffusion Equation Method

In this approach [81], the coupled mode equations are applied to a continuum of modes. If coupling is assumed only between nearest order modes, a particularly simple diffusion-like equation results for mode angle. A Laplace transform permits a number of analytical solutions for various excitation conditions. The evolution of the far-field or the impulse response with length may be studied. The diffusion equation approach is somewhat more physical than the discrete coupled mode equations and gives similar results, though somewhat more easily.

For the step-index case, the variation of the output ring pattern when the angle of an input collimated beam is varied [82] gives rise to a measure of the mode coupling coefficient. More complex theoretical [82] and experimental [83] studies have been made. In graded-index fibers, since the mode number depends upon both angle and radial position, measurements of mode coupling are more complicated [84].

4.4.3 Other Fiber Models

Spectral and chromatic dispersion can be modelled using Equations (4.1) and (4.2) while profile dispersion can be built into a WKBJ model [85]. Models for spectral attenuation are empirical while models for differential mode attenuation are empirical for bound modes [33] and theoretical for leaky modes [49].

4.5 Discussion

Present fiber testing methods have some deficiencies. By concentrating on steady-state excitation conditions, the attenuation methods do not characterize the attenuation transient encountered in the field with real system sources (cut back method). Furthermore, the insertion loss method perturbes the measurement with the uncertainty of a joint loss. The backscatter method introduces uncertainties related to the homogeneity of back scattering centers and the modal power distribution of the backscattered light.

Generally, dispersion is measured under full excitation with the result that measured attenuation and dispersion correspond to different operating conditions. Also, the present methods of dispersion testing do not descriminate fibers that are over or undercompensated.

Of all models of fiber multimode dispersion, the WKBJ method is the most attractive. It is relatively simple and accurate. It can be related to some geometrical optics parameters. This should help the forthcoming research of an adequate description of the modal power distribution launched into the fiber.

5. JOINT CHARACTERIZATION

5.1 Connectors and Splices

Fiber optic transmission systems use two types of fiber joints. Connectors are temporary or demountable joints, while splices are permanent joints.

Connectors offer flexibility in allowing different transmitters or receivers to be linked to different fibers. This flexibility is required for maintenance and repair purposes, as well as for traffic routing and network rearrangement. A fiber optic transmission system may have typically from 1 to 3 connectors per end.

Splices are permanent joints between consecutive sections of fiber. Splices may also be required for fiber repair in a damaged cable. Present cables are typically 1 km in continuous length. With present systems the repeater sections can easily be 10 km long. With due allowance for maintenance and repair splices and for the longer repeater spacing of future long wavelength systems, a repeater section may include up to 20 splices.

With the loss of a connector and a splice being in the order of 1 dB and 0.3 dB, respectively, the joint loss budget might easily be in the order of 12 dB. This is a significant fraction of the total loss budget of a link (approximately 60 dB at the 850 nm wavelength and 45 dB at the 1.3 μm wavelength for a 10 Mbps system).

The large number of joints per repeater section makes it important to know accurately the effect of individual joints since any uncertainty has a cumulative effect from a system point of view.

Fibers can be jointed either with a wet or a dry connector depending on whether or not an index matching fluid is used to minimize reflections at the fiber end faces. Two butted fibers can be permanently spliced either by epoxying them or else by fusing them with a torch or an electric arc [86]. In all cases the fibers are aligned in a fixture whose principle can be likened to that of a V-groove. The fiber claddings are laid under pressure against the surfaces of the alignment fixture in an attempt to control the

fiber transverse offset. Additional optics may be used with connectors to increase the fiber positioning tolerance at the expense of angular tolerance.

5.2 Effect of Joints on System Performance

Joints affect the performance of fiber systems in two different ways. On the one hand, they affect the link loss budget because some optical power may not be transmitted through the joint or guided downstream from the joint. On the other hand, joints affect the link bandwidth (or dispersion) because, through mode mixing, they redistribute the optical power amongst various modes with different propagation speeds.

The loss of a joint is highly dependent upon the distribution of the optical power at the end of the incoming fiber. This is because joints do not attenuate nor couple all modes uniformly.

5.2.1 Intrinsic and Extrinsic Losses

The joint loss consists of two components: an intrinsic loss and an extrinsic loss. The intrinsic loss is caused by the mismatches of fiber parameters like core diameter, NA and index profile. The extrinsic loss is caused by joint impairments like transverse offset of the cores and angular misalignment of the fiber axes. (Some authors use the words extrinsic and intrinsic with the opposite meaning from above.) All above losses are common to connectors and splices. In a connector and in a butt splice, an extrinsic loss is also caused by the longitudinal misalignment of the fibers, by Fresnel reflections at the fiber end faces, and by the tilt of these faces.

In a fused splice an extrinsic loss is also caused by changes in the optical properties of the fused region. The refractive index of the cladding or of the core may change due to the evaporation of the dopants at the melting temperature [87]. The index profile may be altered by the diffusion of the defects. Absorption and scattering within the fused area may also be modified.

Additional defects like air bubbles and fiber bulging or necking at the splice also have a detrimental effect on the splice loss. These latter defects are mostly skill related. They should not be considered as extrinsic causes of loss since normally they can be detected and corrected by resplicing the fiber.

A major contribution to external loss is the transverse offset or misalignment of the core axes. In connectors and epoxied butt splices the transverse offset depends on the accuracy of the alignment fixture (e.g. a V-groove), the cladding diameter mismatch and the core/cladding eccentricity. An analysis of the contribution of the statistical tolerances of the cladding diameter and ellipticity, and of the core/cladding eccentricity has been reported [88]. This involves computing the transverse offset caused by these tolerances when the fiber claddings are laid in a 90°V-groove. A very small average butt-joint loss (0.043 dB) with a 0.1% probability of exceeding 0.33 dB is predicted.

In a fused splice the transverse offset depends further on the self-alignment of the fibers due to the surface tension of the molten glass. This mechanism brings into alignment the claddings. This tends to leave the core/cladding eccentricity as the principal cause of transverse offset. The fusion process and the associated self-alignment have been analyzed in [89,90]. Reduction in misalignment from 4 μm to 0.8 μm is predicted and measured experimentally as a function of the arc duration. The loss of a single mode fiber is computed and measured experimentally.

5.2.2 Local and Transient Losses

Joint losses can also be described in other terms. The joint loss experienced by an operating system has two components: a <u>local loss</u> due to power loss at the joint and a <u>transient</u> loss occuring downstream from the joint in the process of reestablishing a steady state power distribution. Actually, this process results from the combined effects of mode mixing at the joint, and differential mode attenuation and mode cross-coupling in the outgoing fiber.

The fiber parameter mismatches and joint impairments cause a certain amount of mode mixing at the joint. Power in a guided mode of the incoming fiber may be converted into power of the same or other guided modes of the outgoing fiber plus radiating power at the joint and leaky mode power in the outgoing fiber. The radiated power is the local loss. The transient loss is the loss of the outgoing fiber that exceeds the steady state loss.

5.2.3 Effect of Joints on Bandwidth

Because mode mixing takes place at the joint, the power is redistributed amongst various modes. As fibers exhibit differential mode delay the bandwidth (or dispersion) of the outgoing fiber differs from the value corresponding to a steady state power excitation. Actually, the modal power distribution after the splice can be viewed as the modal power excitation of the source for the outgoing fiber.

5.3 Present Testing Methods of Joint Loss

Two methods are currently used to measure experimentally the loss of a joint: the insertion loss method and the backscatter method. The backscatter method is attractive for field use because it requires access to one end of the system only.

5.3.1 Insertion Loss Testing

The insertion loss method consists of measuring the power at the output of the incoming fiber, in jointing the fibers in the field or under controlled conditions in the laboratory, and in measuring the power at the far end of the outgoing fiber. Mode strippers are normally used to remove cladding light.

Because joint losses depend on the incoming power distribution and on the modal characteristics of the outgoing fiber, the measured loss depends on the distances between the joint and both the source and the detector (D_s and D_d respectively) [91]. A short D_d generally results in a smaller loss than a long D_d. The short-D_d loss corresponds to the local loss while the long D_d loss includes the distributed loss as well.

A short D_s generally results in a greater loss than a long D_s. This is because the incoming fiber usually overfills the splice when D_s is short. Some of the modes present with a short D_s are lost at the joint. With a long D_s these modes are not present and do not contribute to the loss.

To measure joint loss under conditions similar to those of an operating system it is preferable to use the long D_s - long D_d combination. The long D_s can be implemented with a long fiber pigtail or else with a controlled launch mechanism (see Section 3.1).

A means of obtaining reproducible joint loss measurements has been presented [92]. This involves launching a steady state power distribution in the transmitting fiber. This distribution is characterized by the 5% width of the far field pattern. A 0.05 dB loss reproducibility requires this width to be controlled within 3%.

The effect of the launch NA (LNA) on splices was studied [4] with 455 m cable 'mode filters' at the input (optional) and output. As the LNA was varied, the input mode filter had the effect of saturating the LNA to the splice to 0.173; for a short 3 m filter the LNA rose to nearly 0.19. The corresponding launch saturations are shown in figure 5.1a. Moreover, the output NA increased 4 to 12% as shown in figure 5.1b. The presence of a splice was shown to increase by 0.1 dB the average 7.7 dB loss of the output mode filter fibers.

Love [7] also demonstrated theoretically and experimentaly the importance of a steady state distribution, created by a bend in an input fiber, to the measurement of imperfect splices.

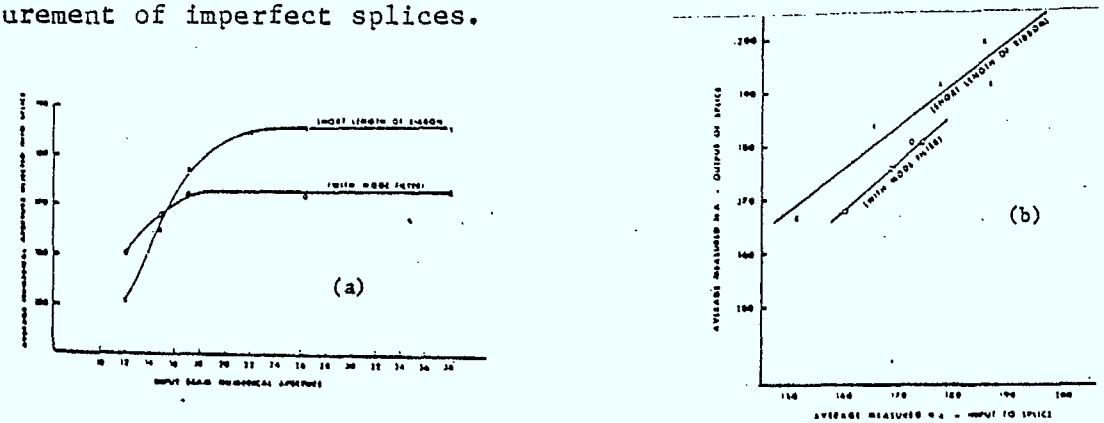

Figure 5.1 NA at Filter Output (a) and at Splice Output (b) versus LNA into Filter for 3 m and 455 m Filter

5.3.2 Backscatter Testing

The backscatter method requires a more sophisticated test set-up than the insertion loss method. Furthermore, the results of this method are difficult to interpret, yielding a substantial uncertainty in measurement accuracy.

For convenience and mostly for lack of a better model, the total loss of a joint (L_m) measured by the backscatter method is simply assumed to be half of the power drop observed on the backscatter scope trace at the joint location, i.e.

$$L_m \text{ (in dB)} = -5 \log (P_o/P_i) \tag{5.1}$$

where P_o and P_i are the power levels after and before the joint [93]. This is a crude approximation since the observed power drop is a combination of the losses in the forward and in the reverse direction:

$$L_{bs} = L_{\ell f} + L_{\ell b} + L_{tb} \tag{5.2}$$

where $L_{\ell f}$ and $L_{\ell b}$ are the local losses in the forward and the backward direction respectively. L_{tb} is the transient loss in the backward direction. Eq. (5.2) differs from the actual loss L_s seen by the operating system:

$$L_s = L_{\ell f} + L_{tf} \tag{5.3}$$

where L_{tf} is the transient loss in the forward direction. Averages of the joint losses measured by the backscatter method from the two ends of the joint have been used [94,95].

The intrinsic losses due to a mismatch in fiber parameters are not the same in the forward and in the reverse directions. Furthermore, the power distribution exciting the joint in the forward direction is generally in

steady state (long D_s) while the power distribution in the backward direction is closer to uniform because of the mode mixing action of the joint.

The peculiarities of the backscatter are such that, under certain combinations of NA, core diameter, fiber attenuation and backscatter, an apparent gain is observed on the backscatter trace [95]. This makes joint loss interpretation difficult. Even when the scope trace shows a real loss, the same phonomena lead to uncertainty in the actual value of the joint loss.

5.4 Present Testing Methods of Mode Mixing at Joints

Until recently the testing of the joint performance was concerned with loss. However, the performance of joints has now been investigated on a global basis, i.e. from a total link point of view. This is discussed in Section 6. A few experiments on mode mixing at joints have also been reported.

"Mode movement" defined as the relative power variation at a particular angle in the far-field pattern has been demonstrated experimentally [96]. This study compares the mode movement, which is equivalent to mode mixing, in a fused splice and a butt joint with index matching fluid. For a given loss it appears that fused splices exhibit a greater mode movement than butt joints. This illustrates that mode mixing takes place in the fused area.

A similar conclusion is reached in [97] where it is shown that a butt joint introduces less mode mixing and less differential mode delay (DMD) equalization than a good fusion splice. In turn, the latter introduces less mode mixing than a high loss fusion splice. The measurement of the DMD of two fibers individually and after splicing indicates that the DMD of the link depends very much on the DMD of the last fiber.

With coherent sources, splice loss depends also on wavelength [98]. This topic would be relevant to a study of modal noise induced by a joint.

5.5 Joint Models

Most joint models address the question of a butt joint with index matching. They correspond to idealized connectors or to epoxy-splices. Changes in the refractive index of the fused zone have also been considered [99].

Two main approaches are used for joint modelling: a geometrical optics or ray approach and a field theory approach.

5.5.1 Geometrical Optics Models

A geometrical optic model predicts the intrinsic losses of the joint as the sum of the losses due to NA, core diameter (d) and α-profile mismatches

$$L = -10 \log (d_o/d_i)^2 - 10 \log (NA_o/NA_i)^2 - 10 \log (\alpha_o(\alpha_i + 2)/\alpha_i(\alpha + 2))$$

when $d_o \leq d_i$, $NA_o \leq NA_i$ and $\alpha_o \leq \alpha_r$.

The subscripts i and o refer to the incoming and outgoing fiber, respectively. This simplistic model is based on the ratio of the maximum number of modes supported by the outgoing and incoming fibers, respectively [100]. It assumes a uniform power distribution, no differential mode attenuation and no cross-coupling.

Another model determines the number of incoming rays or modes that are accepted by the outgoing fiber. The acceptance criterion is that the ray be contained within the local NA of the outgoing fiber. This involves computing the ratio (NA_o/NA_i) for all points of the overlap area of the cores. The loss at each point is then weighted by the incoming power distribution. The model initially assumed the power to be uniformly distributed within the local NA and across the core [101]. Subsequent refinements to this model assumed a Gaussian power distribution within the local NA and a steady power distribution across the core: $p(r) = (1 - r^2)^2$ for a parabolic profile [102,103]. The Gaussian assumption is essentially empirical. It is meant to reflect implicitly the existence of differential mode attenuation. The same concept underlies the choice of a steady state power distribution.

This Gaussian model is powerful enough to evaluate the local loss due to core diameter, NA and α-profile mismatches, and to transverse offset and eccentricity. To model the distributed loss, it is assumed that one half of the power falling outside of the outgoing local NA is lost in the process of reestablishing the steady state power distribution downstream from the joint.

Leaky rays and mode coupling are not treated explicitly so that the approach is rather qualitative. It can not easily be used in a global model that would determine the impact of joints on bandwidth.

The above model has been used, perhaps erroneously, to compute the splice loss as measured by the backscatter method [104]. Indeed, the assumptions of the Gaussian model may not be met in the backscatter method. The method was used to establish a correlation between backscatter loss and local (forward) loss. The backscatter measurement was determined as the best estimator of the local loss. However, the correlation is weak (56%).

Under the assumption of uniform modal power excitation, the intrinsic joint loss has been modelled as the ratio of the mode volume common to both fibers over the mode volume of the incoming fiber [105]. After extensive statistical simulations and regression analysis analytic expressions for the statistical loss distribution have been determined.

A butt fiber joint has been modelled using the WKBJ approach [106] for α-profile fibers with a transverse offset. A mode transfer matrix is computed by summing the contributions of all propagating modes whose propagation numbers correspond to a solution of Snell's Law. When the two fibers are identical, modes with mode number m_1 excite modes with mode number m_2 where $m_2 = Md\ (d - 2r\cos\Theta)$. M is the maximum number of guided modes and d is the transverse offset; Θ and r are the polar coordinates on a point of the incoming core in the overlap area of the cores. Theoretical and experimental results show the modal power distribution before and after the splice for a 0.5 relative offset.

The relation between transverse offset and the impulse response is also considered [106]. The impulse response of the lower and higher order mode

groups is obtained through annular filtering of the far field pattern. The differential delay between these mode groups is shown to decrease with increasing offset when both fibers are identical (see Figure 5.2). However, when an overcompensated fiber is butt jointed to an undercompensated fiber the differential delay increases with transverse offset from its mimimum value at zero offset. A joint does not always improve the link dispersion. The model has been used to predict the 3 dB bandwidth of a 2.2 km fiber link. Good agreement with measured bandwidths is obtained for relative offsets greater than 0.2. Discrepancies for smaller offsets could be due to the departures of fibers from the ideal α-profile. Also, leaky rays are not accounted for.

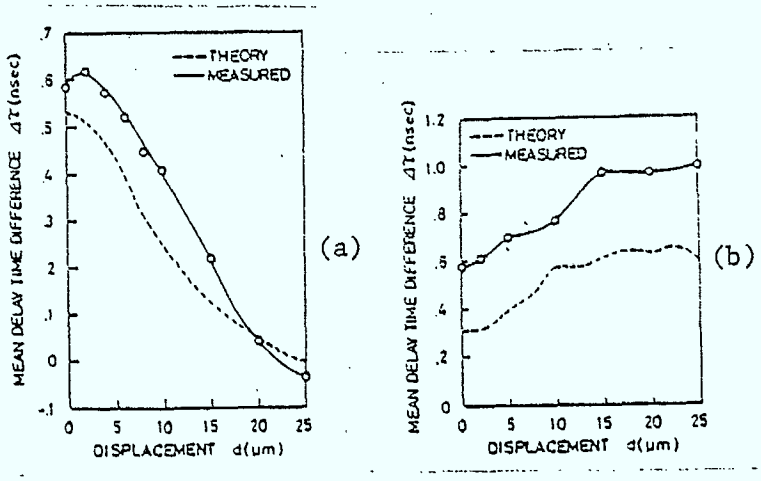

Figure 5.2: Effect of Transverse Offset at Joint on Mean Delay Time Difference Between Lower and Higher Order Modes for Two Identical Fibers (a) and a Particular Combination of Different Fibers.

5.5.2 Field Theory Models

The common principle of the models based on field theory is to expand the incoming field at the joint into a sum of the propagating and radiating modes of the outgoing fibers. Generally, a cross coupling matrix is determined using the orthogonality property of the fields. The effect of the splice on impulse response or bandwidth is computed. In this case, the fibers are assumed to have an α-profile so that the WKBJ modal transit times can be used.

The reflection from a tilted fiber end face has been modelled by expanding the reflected field into a Laguerre polynominal after integration of the Hermite polynominal in the field of the idealized modes of a parabolic fiber [107]. It

is shown that when all guided modes are equally excited by an incoherent source a step index fiber loses 50% of its power when the end face is tilted by a 3.75° angle. This loss is on top of the reflection loss at the fiber/air interface. No experimental verification is provided.

The joint loss of identical parabolic fibers has been considered as a function of fiber tilt and lateral offset [108]. The analysis is based on a field expansion in terms of Hermite Gaussian functions. The model was used to compute the cumulative effect of a large number of consecutive splices 20 cm apart. The initial excitation is either uniform or consists of a plane wave. It is shown that, as the number of splices increases, the far-field pattern and the splice loss become independent of initial excitation conditions. Good experimental agreement is demonstrated in the case of the far-field pattern. The pulse broadening of a concatenated link of length L made up of 1 km fiber sections is shown to vary as L without transverse offset and to tend towards $L^{\frac{1}{2}}$ when the offset increases towards 30% of the core radius. It is not clear how the differential delay was modelled. Leaky modes were neglected and presumably so was the differential mode attenuation. The study is of theoretical nature only.

Fiber dispersion versus transverse offset at the joint has been investigated [109]. The fields are expanded in terms of Gauss-Laguerre functions for graded-index fibers and in terms of Bessel functions for step-index fibers. Differential mode attenuation and mode mixing are disregarded. Differential delay is computed using the WKBJ approximation. The RMS dispersion is predicted to increase by about 10% when the transverse offset increases to about 80% of the core radius. Greater offsets reduce rapidly the dispersion. The amplitude corresponds to uniform modal power excitation at the joint. The amplitude of the increase is shown to depend largely on the modal excitation of the joint. The agreement between the computed and measured RMS dispersion is only fair. This can very likely be attributed to the idealistic assumption of α-profile and to the non-uniform modal power excitation.

The relation between joint loss and transverse offset has been discussed with the aid of a field decomposition into reflected and transmitted field components [110]. The resulting power reflection and power transmission matrices were computed and applied to the cases of single mode fibers and multimode step-index fibers with either uniform or steady-state modal excitation.

This method was generalized to treat fibers of arbitrary index profile [111]. The profile is approximated by a staircase. Propagation matrices define the fields within a profile step region. Boundary matrices relate the fields of adjacent layers. The method was used to compute the offset loss and the tilt loss of step- and parabolic-index fibers, and of dual-mode fibers.

A fused splice has been specifically modelled by considering index profile perturbations over the fused length: a half-period sinusoidal variation along the splice axis and a 4-th order polynominal variation in the radial direction [99]. The parabolic index fibers are assumed identical without transverse offset. Using a Laguerre-Gaussian field expansion, numerical computations determine the mode coupling coefficients, the dependency of splice loss on the length of the fused region and on the incoming modal power distribution, and the bandwidth increase with the percentage of mode conversion. The mode conversion is defined as the total converted power, including lost power, divided by the total guided power. The modal power distribution is assumed of the form $(m/GM)\exp(1 - m/GM)$ where m and M are the mode number and the number of guided modes, respectively, and G is a parameter. Power coupled to leaky modes is not considered here.

5.6 Discussion

Joint loss has two components: a local loss and a transient loss. Both components depend on the modal excitation of the joint. Furthermore, the transient loss is related to the differential mode attenuation of the downstream fiber. Mode mixing at the joint impacts on the fiber bandwidth via the fiber differential mode delay.

Because of the modal behaviour of joints, present testing methods are deficient. In the insertion loss method the modal excitation generally differs from the modal power distribution seen by joints of operational links. In the backscatter method the joint loss measurement is also directly affected by the forward and backward modal scattering properties of a long length of upstream fiber.

Presently mode mixing at the joint is rarely measured although it may impact significantly on the fiber link bandwidth.

Of the theoretical joint models, the WKBJ approach is most conducive to the inclusion of modal power distribution. Furthermore, it is compatible with a WKBJ model of the fiber.

6. CONCATENATED FIBER LINK CHARACTERIZATION

This section deals with the length evolution of attenuation and dispersion in a fiber system. It reviews transmission (attenuation and dispersion) measurements on concatenated fiber links. The several classes of concatenation are not always distinguished in reports. Fibers may be:

- uniform or nonuniform along their length (to within a tolerance)
- identical or non-identical to each other (to within a tolerance)
- equal or unequal length.

The complexity of transmission link types can vary all the way from behaviour along a single uniform fiber up to behaviour along jointed nonuniform unequal lengths of fibers. Because of variations in the fiber manufacturing process and in installation practices, usually this last case is attained. With technological improvements, however, fibers will become more uniform and identical, and transmission behaviour along a concatenated link may be easier to describe.

6.1 Attenuation Versus Length

Early system installations have generally shown that the overall attenuation of a link has a value less than the sum of the specified attenuations of the individual fibers. Sometimes the discrepancy was attributed to uncertainty in splice measurements, with link deviations giving anomalously good or bad splices; however, negative splice losses are often obtained. It was soon realized that attenuation non-additivity was probably due to the fact that although individual fibers at that time were characterized using nearly full-mode source excitation, this condition was usually not duplicated at the fiber input, and certainly not at subsequent joints. Although the resultant attenuation discrepancy could be forgiven in early systems, it was clear that cost-effective fiber utilization would require more accurate concatenation prediction. Moreover, the methods of measuring fiber and joint attenuations

must be consistent with each other.

The first reported study [18] of attenuation rate vs single fiber length was in 1975. Fiber lengths of 4 km were progressively cut back while the throughput power was monitored. Even though the attenuation of each cut off section was measured using the same 0.1 launch NA as was used on the full length, an excess attenuation was noticed for about the first 1-2 km.

6.1.1 Effect of Spectral Width of the Source

The first published study of attenuation rate along a concatenated link is only three years old [112] and was based on a BPO installation. A restricted LED launch condition launch NA = 0.13 (70% of the 0.18 fiber NA) and launch spot = 25 μm (40% of the 60 μm core) was used. The attenuations obtained in this way summed to about 24.4 dB over each of 4 fiber channels of 5.75 km, and the concatenated results measured to within 0.1 dB of this value. No account was taken of the 5 joint losses estimated to be about 0.2 dB each. It was thought that this might be due to the fact that with a spectrally broad LED, the wings of the spectrum attenuate about 0.15 dB within the first 1 - 2 km, so that this number should be subtracted from the individual attenuations of each succeeding section. This spectral filtering complication will presumably be absent with laser sources.

In an NTT study [6,9], the attenuation of individual fibers was determined by using an LED with a 500 m dummy fiber V-groove spliced onto each test fiber; a 2 m cutback length was used. When the attenuations were measured this way for 12 fibers, the column (1) of Table 6.1 was generated. The fibers were then spliced into a 5 km link and then progressively cut. Column (2) is the optical loss between a cut just before the splice and a cut 2 m after the next splice closer to the source. The measured splice loss of column (4) represents the loss between cuts just before and 2 m after the splice. The 'predicted' splice loss column (3) is theoretical and of little interest here except to note that the higher measured values were attributed to poor assembly. Note the small difference (1) minus (2). In correlating with a later field measurement, an assumed splice loss was used.

Fiber no.	(1)[a] Optical loss (dummy fiber method) (dB)	(2)[b] Optical loss (measured for spliced fiber) (dB)	(1)–(2) Difference (dB)	(3) Splice loss (predicted) (dB)	(4)[c] Splice loss (measured) (dB)
1	1.58	1.59	−0.01	0.47	0.51
2	1.64	1.75	−0.11	0.66	0.61
3	1.57	1.51	0.06	0.15	0.28
4	1.59	1.52	0.07	0.27	0.26
5	1.62	1.71	−0.09	0.25	0.21
6	1.56	1.55	0.01	0.40	0.41
7	1.59	1.59	0	0.35	0.23
8	1.48	1.58	−0.10	0.11	0.52
9	1.46	1.44	0.02	0.34	0.19
10	1.53	1.56	−0.03	0.14	0.52
11	1.48	1.56	−0.08	0.23	0.53
12	1.70	1.60	0.10		
Average	1.57	1.58	−0.01	0.31	0.39

[a] Dummy fiber length and cut length are fixed to 500 m and 2 m, respectively.
[b] Cut length is 2 m.
[c] Splice loss is estimated at 2 m after the splice point.

Table 6.1 Comparison Between Individual and Spliced Fiber Losses at NTT

6.1.2 Restricted Launch Conditions

A test of several tungsten lamp/monochromator launch conditions was undertaken [113] on a 0.18 NA 45 μm core fiber:

a) an overfilled launch with a 25 m tightly wound reference length,
b) overfilled with a 1 m reference length, and
c) a 55% NA and a 65% spot with a 1 m reference.

These were compared with a GaAlAs laser-driven 11.7 km link including 9 splices which had a total loss of 44.9 dB. The sums obtained (without splice losses averaging 0.3 dB) are 44.5 dB for (a), 52.2 dB for (b), and 44.7 dB for (c). It was confirmed that 0.7 out of 0.8 dB was due to a transient loss over the first 100 m of one fiber. Moreover, (c) produced narrower near-field and far-field patterns than (a); it was thought theoretically that lossy higher-order guided modes rather than leaky modes contributed to transient loss.

A similar BPO test [114] used:

a) an overfilled launch (LED),
b) a 40% NA, overfilled spot (arc lamp and filter), and
c) a 40% NA, 50% spot.

A cumulative probability distribution as in Figure 6.1 showed that balancing of the differences about zero would occur if something between (b) and (c) were used. Joint loss 'prediction' was not reliable.

A rather random Italian study [21] of several fiber types and laboratories found that a 40 μm spot, 0.12 NA gave consistency (and agreement with backscatter values).

6.1.3 Effective Mode Volume

The effective mode volume (EMV) concept described in Section 3.1.4 has been used to generate an EMV transfer function for each fiber (and possibly, joint) prior to concatenation [115, 116]. This consists of a plot of output EMV vs input EMV as in Figure 6.2a for a fiber with and without microbending. The full launch fiber EMV appears to be about 140, although this is not strictly comparable to the 3 dB definition. Secondly, a plot of attenuation vs input EMV is generated as in Figure 6.2b for the same fiber. (Both these plots are presumably length-dependent). The source EMV (assumed circularly symmetric) input to the first fiber yields the attenuation and output EMV for that fiber. A 2.7 dB loss difference was observed between an LED and an ILD. Across the splice the EMV may increase by about 0.4. The resultant output EMV becomes the input EMV to the next section, yielding its attenuation and output EMV. The process is continued over all sections and the attenuations are summed. For three 1 km lengths and link input EMV's ranging from 2 to 35, the resulting attenuations from 0.9 to 1.8 dB/km at 1.2 μm were predicted to within 0.07 dB/km. This has recently been extended to 10 km [117] with variable launch conditions giving a 18-23 dB link loss, for a prediction accuracy of 0.5 dB.

Admitting that this characterization is somewhat complex, this work recommended that for these fibers an injected EMV of about 9 would most nearly approximate long-length results. Source deviations could be accounted for by a positive or negative transient loss.

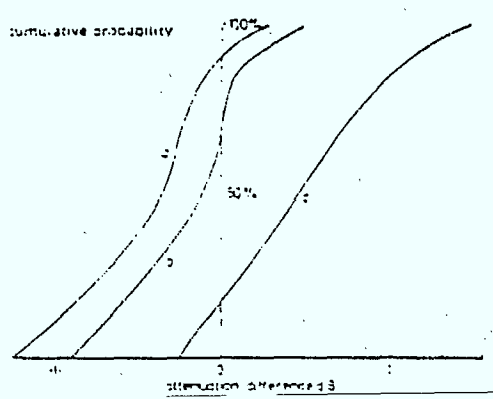

Figure 6.1 Distribution of Attenuation Differences Between Isolated Cables (Launch Conditons a,b,c) and Jointed Cable.

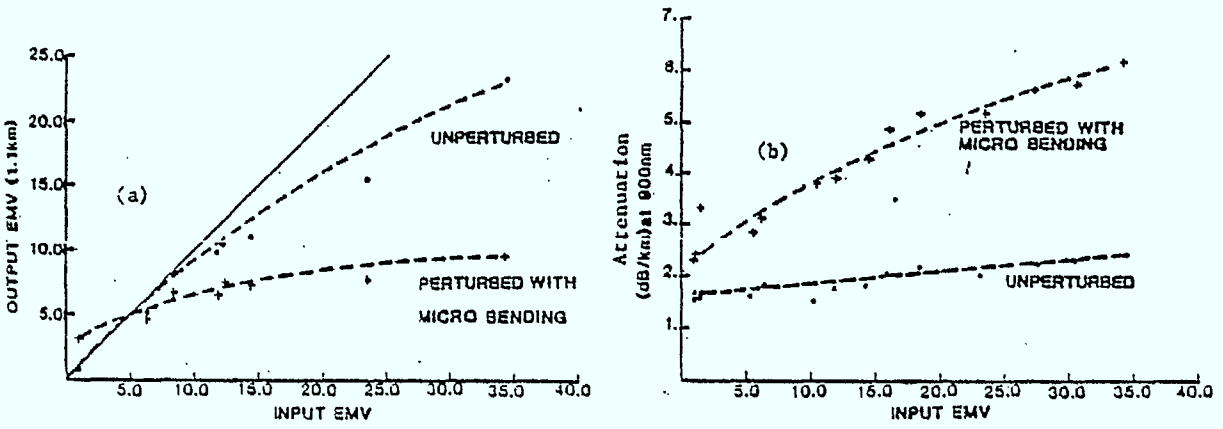

Figure 6.2
Output Effective Mode Volume (a) and Attenuation (b) Versus Input EMV With and Without Microbending.

6.2 Dispersion Versus Length

6.2.1 Multimode Dispersion

6.2.2.1 Multimode Dispersion in Time Domain

The earliest reported measurements of dispersion vs length were made in 1973 on Corning Glass Works - Bell Telephone Laboratories (CGW-BTL) graded index fiber [118]. The FWHM vs length result is shown by the log-log plot of Figure 6.3. From interference measurements, the fiber profile was asymmetrically donut-shaped with an NA of about 0.10 and an attenuation of 13 dB/km at 900 nm. Its 1 km length was measured with 3 sources. The He-Ne laser at 633 nm and the ND:YAG laser at 1060 nm gave roughly square-root-of-length pulse spread dependence, particularly at shorter lengths. A 2 km result at 633 nm was obtained both by recording a pulse returning from one round trip with the fiber end immersed in a mercury end reflector and also by splicing on another km of very similar fiber. A GaAs 900 nm source showed the root length dependence

only above 550 m of fiber; below that the length behaviour was linear. This was tentatively attributed to a difference of launch conditions here consisting of a very elliptical input pattern.

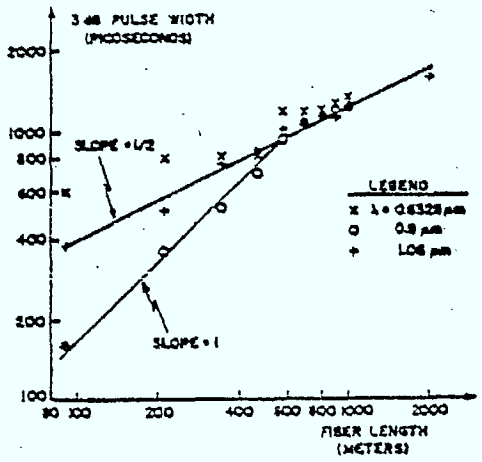

Figure 6.3
Half-Power Output Pulsewidths Versus Cut Fiber Length at Three Wavelengths. The Longest Length Corresponds to a Splice.

An Italian installation [119] of CGW fiber in an 8 km CSELT cable produced a ns FWHM pulse broadening that (by our calculations) went as $0.36\ L^{-0.8}$. It is interesting that the broadening-times-bandwidth product at 1,2,3,4 and 8 km gave 380,390,410,440 and 450 indicating an approach at longer length toward the Gaussian value of 440.

Some interesting results on low loss (7 dB/km at 840 nm) silicone coated silica fiber [120] were interpreted with the mode diffusion equation utilizing strong mode coupling and differential modal attenuation. 'Quasi-steady state' was defined as having fiber characteristics (far-field, bandwidth, attenuation) independent of launching NA; it occured for about 120 m in this case. Between 120 m and 2.5 km, the bandwidth decreased as $L^{-0.7}$ whereas past 2.5 km it reached the 'true equilibrium' variation of $L^{-0.5}$.

a) Shuttle Pulse Method

Shuttle-pulse measurements on a 106 m fiber section with mirrors at each end (see figure 6.4) were reported in [121]. Fiber length could thereby be

extrapolated to any odd number of pulse traverses, 19 in this case for an effective length of 2014 m. Data showed some disagreement with the measurement in [118] and it was thought that fiber length nonuniformity was a problem. The effect of mode-mixing was also investigated as the fiber was unwound from a 30 cm diameter drum (circles on Figure 6.5). The squares represent readings taken when the fiber was unwound onto a flat surface with many overlaps and twists present. This increased the attenuation by 4 dB/km while it reduced the pulse broadening. The opposite effect is shown by the triangular points in which the fiber was rewrapped onto an untwisted 60 cm spiral. These results agreed well with theory [80] in which the excess attenuation loss A (in dB) is related to the fractional improvement F in pulse broadening:

$$A.F = 0.4 \qquad (6.1)$$

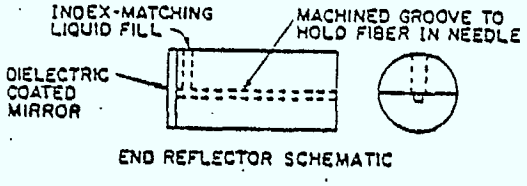

Figure 6.4
Fiber Mirror Used in Shuttle-Pulse Measurements

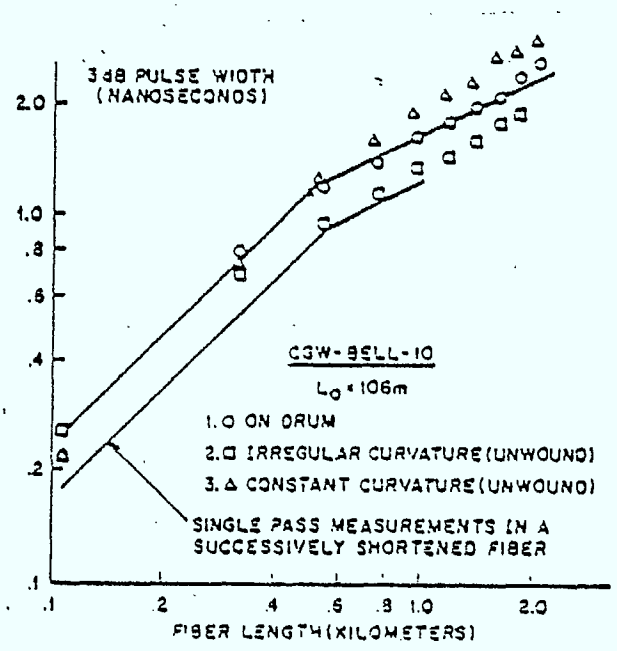

Figure 6.5
Pulsewidth Versus Fiber Length Via Shuttle-Pulse for Three Winding Arrangements

A longer length quasi-step-index fiber (loss 6 dB/km at 0.9 μm, NA = 0.16) was extrapolated from 1.28 to 6.4 km via the shuttle-pulse method [122]. Unlike the examples discussed above, this showed a more gradual transition from slope 1 to slope 1/2 as in Figure 6.6. A coupling length

L_c = 840 m was deduced. Pulse shapes after 3 traverses (3.84 km) were independent of launch conditions. From these measurements and the above, we can deduce a simple description of pulse broadening T vs fiber length L (in km):

$$T(L) = T(1)L \qquad L \leq L_c \qquad (6.2)$$
$$= T(1)\left(L_c L\right)^{\frac{1}{2}} \qquad L \geq L_c$$

Measured impulse responses were Fourier-transformed in this work [122] to yield the baseband response functions of Figure 6.7. A Gaussian fit to the amplitude rolloff improved with longer lengths while the phase shift for a given rolloff decreased (indicating greater symmetry in fiber impulse response).

Still further shuttle-pulse measurements [123] on lower loss (2.3 dB/km at 900 nm) fiber enabled an extrapolation from 0.15 to 2.5 km in Figure 6.8. For this low mode-mixed case, a linear slope dependence was found at both 3 dB and 10 dB widths. Moreover, pulse shapes were sensitive to off-axis excitation. Both these observations showed that the coupling length was in excess of the 2.5 km.

b) Pulse Circulation Method

A second length-extrapolation technique is a pulse circulation method in which an ultrasonic deflector is used to deflect and relaunch into a loop of fiber [124]. About 3 fiber lengths improvement over the shuttle pulse method was obtined; 5 km were measured. Two step-index fibers with about an 8 ns pulse spread at 1 km had an $L^{0.5}$ dependence which was preserved as $L^{-0.5}$ for the 3 dB bandwidth. However, graded index fiber started from 0.4 ns/km at 1 km and increased as $L^{0.85}$ in broadening and

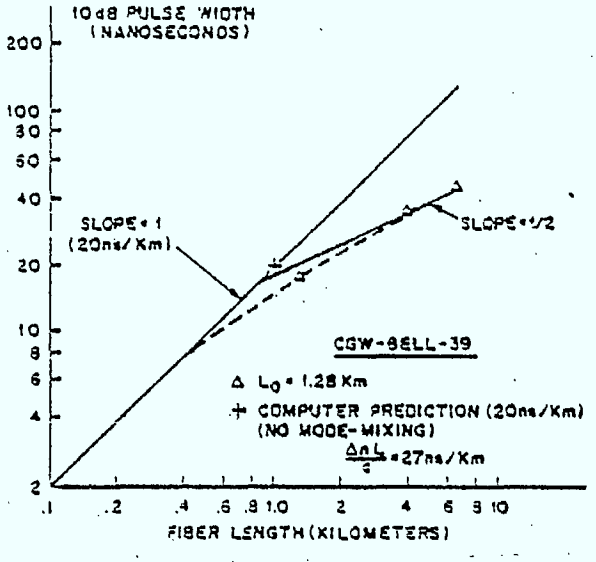

Figure 6.6
10-dB Pulsewidth Versus Fiber Length Via Shuttle-Pulse to 6.4 km. Note the More Gradual Slope Decrease.

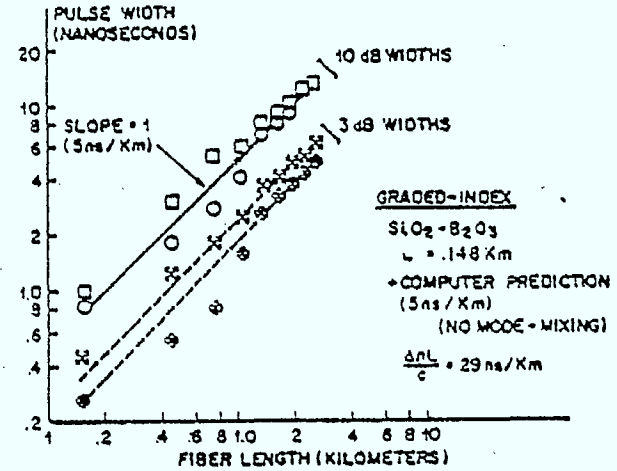

Figure 6.8
3-dB and 10-dB Pulsewidth Versus Length in Shuttle-Pulse Measurements.

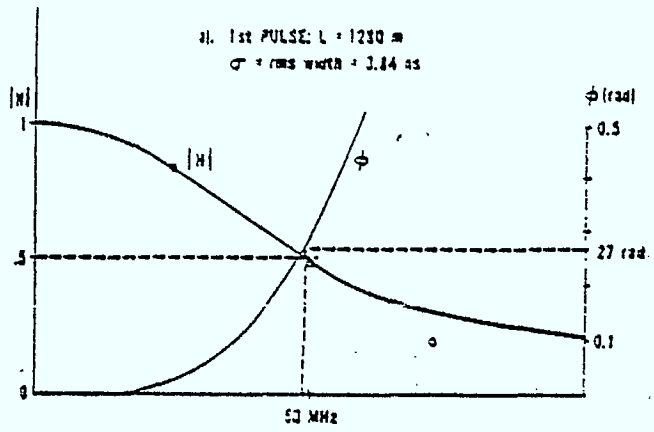

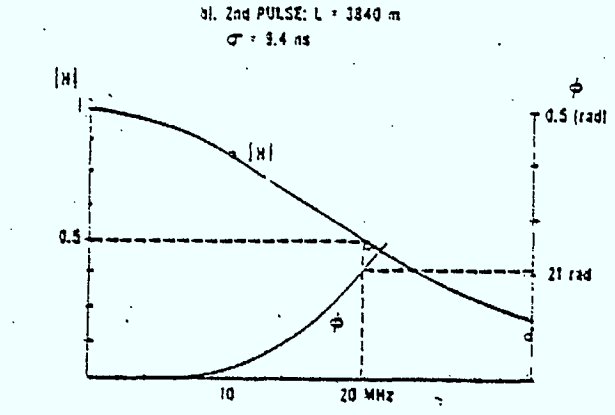

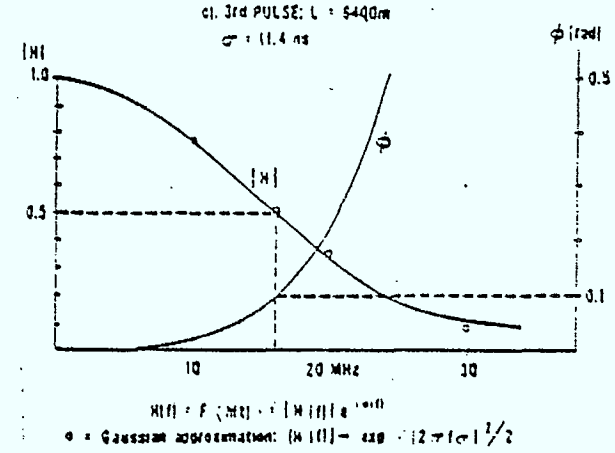

Figure 6.7
Baseband Frequency Responses Obtained from Fourier Transforms of the Pulses of Figure 6.3.

$L^{-0.7}$ in bandwidth. The latter discrepancy was attributed to material dispersion which is proportional to L. Here a 847 nm laser was used with a 1.3 nm spectral FWHM, so, as in Figure 6.9, correcting for material dispersion reduced the multimode dispersion term to an $L^{0.75}$ variation. Clearly, a length near 4 km existed beyond which chromatic dispersion exceeded multimode dispersion.

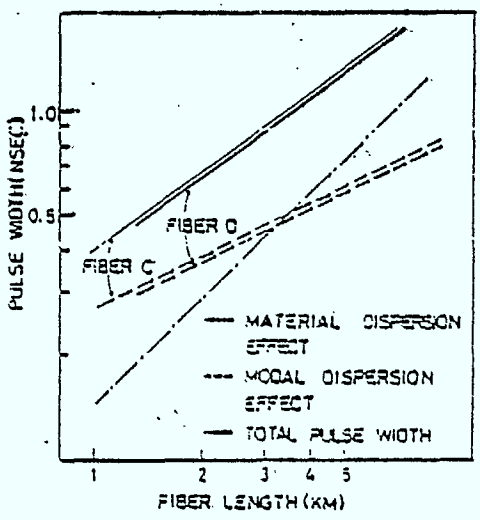

Figure 6.9
Pulsewidth Versus Length for Low Dispersion Fiber. Multimode and Chromatic Dispersion Components Are Separated Out.

6.2.1.2 Multimode Dispersion in Frequency Domain

Frequency domain measurements on spliced lengths of fiber were first carried out in France. Log-log plots of 3 dB bandwidth vs. fiber length showed a slope varying from 0.6 to 1.4 depending upon launch conditions from GaAlAs or YAG sources [125]. The phase derivative showed that the group delay was virtually constant with modulation frequency. It was found that a Gaussian model, in which the roll-off with modulation frequency f is given by $\exp\{-(f/f_n)^2\}$ for the nth fiber, was closely followed [126]. The overall bandwidth B is obtained from

$$B^{-2} = \sum_n f_n^{-2}, \quad \text{or } B = B(1)\, L^{-\frac{1}{2}} \tag{6.3}$$

for identical fibers of equal lengths. Typical results, in which the individual bandwidths varied from 390 to 790 MHz, are shown in Figure 6.10.

The frequency domain scheme was later extended to accomplish multiplication of transfer functions by first doing measurements on individual fibers with the mode scrambler of Figure 3.4 [11]. Figure 6.11 shows the transfer functions of two step-index fibers measured singly and also V-groove spliced together. The calculated product (i.e. dB summation) shows very good agreement. The plot in Figure 6.12 shows a linear variation of dB roll off with length, but with an increasing slope with higher modulation frequencies. Discrepancies of dB addition at longer lengths were attributed to intermodal phase effects since only mode amplitudes are controllable by the mode scrambler.

In another study [2,127] four rather dissimilar graded-index fibers were used. With direct excitation from the injection laser diode, transfer function multiplication underestimated rolloff for the concatenated link. Bandwidth was expected to decrease inversely with length, but this overestimated the rolloff. Next, the steady-state mode exciter of Figure 3.1 was used on individual sections, and moreover, the mode scramblers of Figure 3.2 were loaded after each splice. Excellent agreement of measured and multiplied values was found. Moreover, the scramblers gave a 3-fold improvement in bandwidth at a loss penalty of 0.15 dB per splice.

Concatenation bandwidth measurements were made on some VAD (vapor-axial deposition) fiber [128] and fit to an expression of the form

$$B = \left(\sum_n B_n^{-1/\gamma}\right)^{\gamma} \tag{6.4}$$

where B_n is the bandwidth of the nth fiber before splicing and γ is a parameter. It was found that $\gamma = 0.6$ provided a reasonable fit. Other more detailed measurements [6] showed that γ decreased with increasing fiber length to about 0.55, and also had a distribution about this mean value.

It was speculated that although it might normally range from 1/2 to 1, γ could be smaller or even negative due to equalization effects. It is

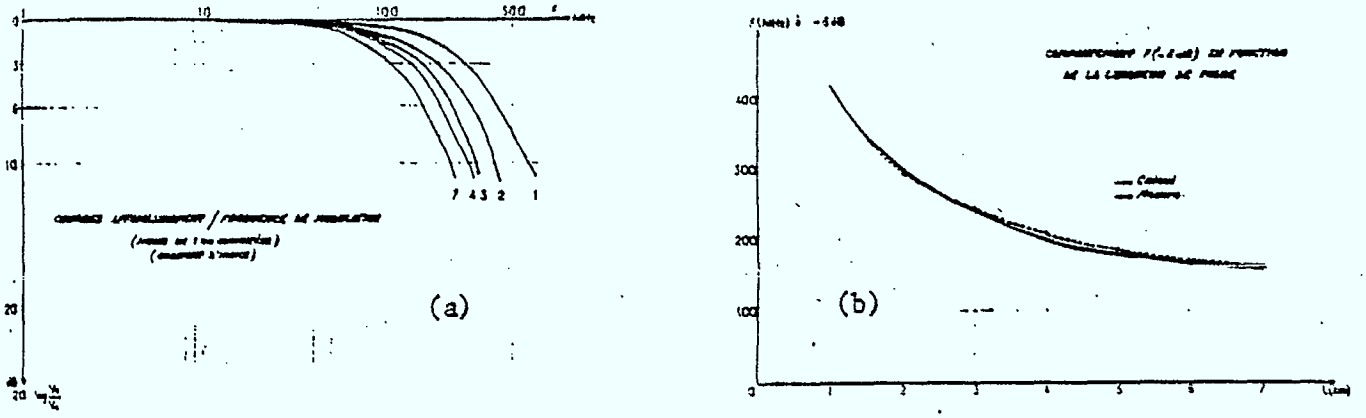

Figure 6.10: Transfer Function (a) and 3 dB Optical Bandwidth (b) Versus Fiber Length.

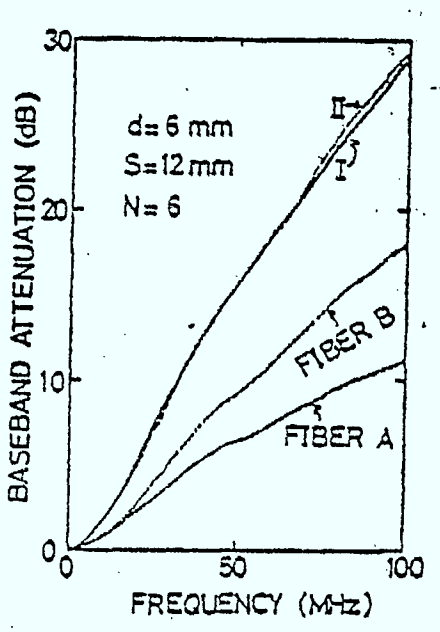

Figure 6.11
Baseband Response Function for Two Fibers Along With the Logarithmic Sum (II) and the Measurement (I) for the Fibers Spliced. Mode Scramblers were Used.

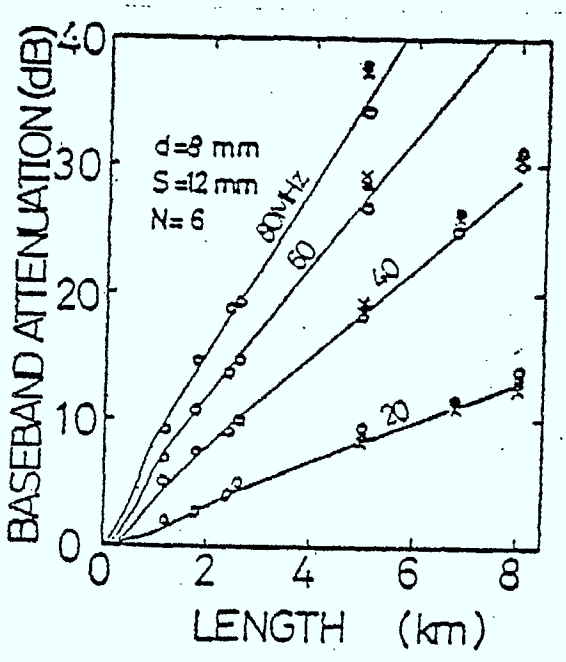

Figure 6.12
Length Dependence of Baseband at Several Frequencies.

noteworthy that extremely long lengths of such fiber have been concatenated [129]. Sections ranging from 11 to 30 km have been spliced into links of 65 km (λ = 1.3 μm, loss 37 dB, bandwidth 36.5 MHz) and 116 km (1.55 μm, 35.2 dB, 16.5 MHz). Details of individual section performance were not given.

6.2.2 Modal Delay Equalization

6.2.2.1 Effect of Mode Mixing and of Splices

The dependence of pulse broadening on the square root of length had been predicted early [55] as due to mode coupling. Such coupling is strong when scattering imperfections along a guide are spaced one mm or less apart, corresponding to the reciprocal phase velocity differences of the modes. Coupling from bound to unbound modes was also predicted to lead to loss along with possible orders of magnitude improvement in fiber dispersion. Today we know that too large a loss penalty is suffered for induced mode mixing in return for only modest gains in dispersion.

It was later recognized that in addition to launch effects, splice effects should be considered in any link concatenation. In one detailed experiment [130] two 1.35 km lengths of radically different fibers were used; one had heavy mode mixing (as determined by the insensitivity of output pulse to input launching) and a 1.02 ns broadening whereas the other had light mixing and 4.1 ns broadening. Differential micropositioners were used to adjust both transverse and longitudinal offsets at the splice, and changes in FWHM pulse widths were measured. With light travelling from the first fiber to the second, the pulse broadening increased to almost 4 ns with a transverse offset of 2/3 times the core radius (30 μm); beyond this the broadening decreased and actually became minus 1 ns for a 1.5 times offset (Figure 6.13). The effect of longitudinal displacement is shown in Figure 6.13b.

With light going from the lightly mode mixed fiber into the heavily mixed one, the transverse and longitudinal displacements produced the effects of Figures 6.14 a,b. The greatly reduced dispersion is expected since the

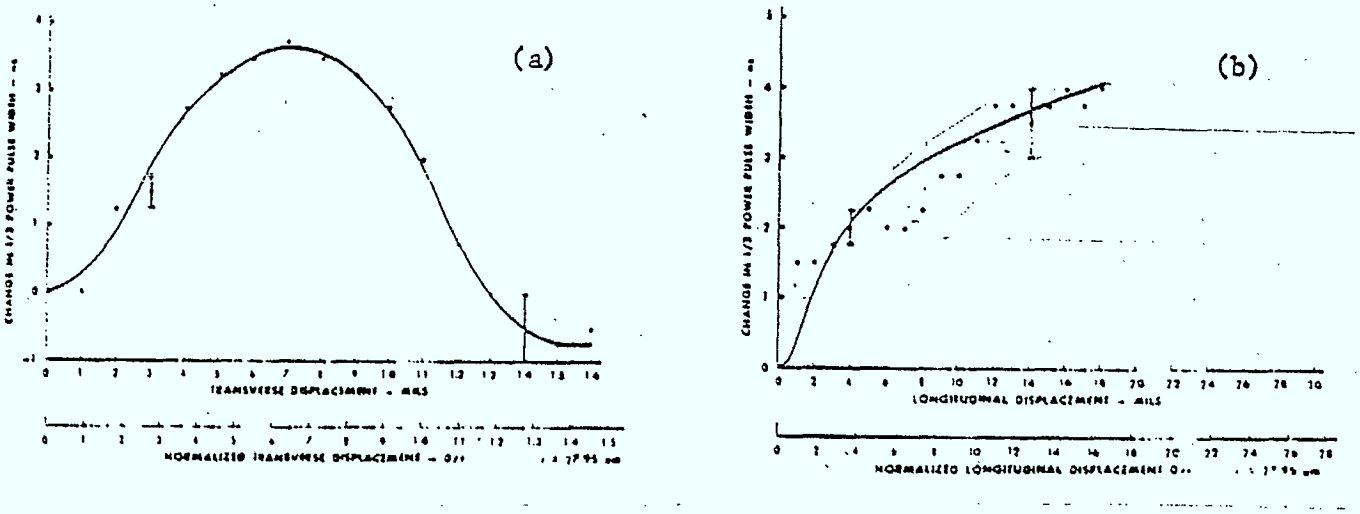

Figure 6.13: Change in Pulse Broadening Versus Transverse (a) and Longitudinal (b) Offsets With the Transmitting Fiber Heavily Mode-Mixed and the Receiving Fiber Lightly Mixed.

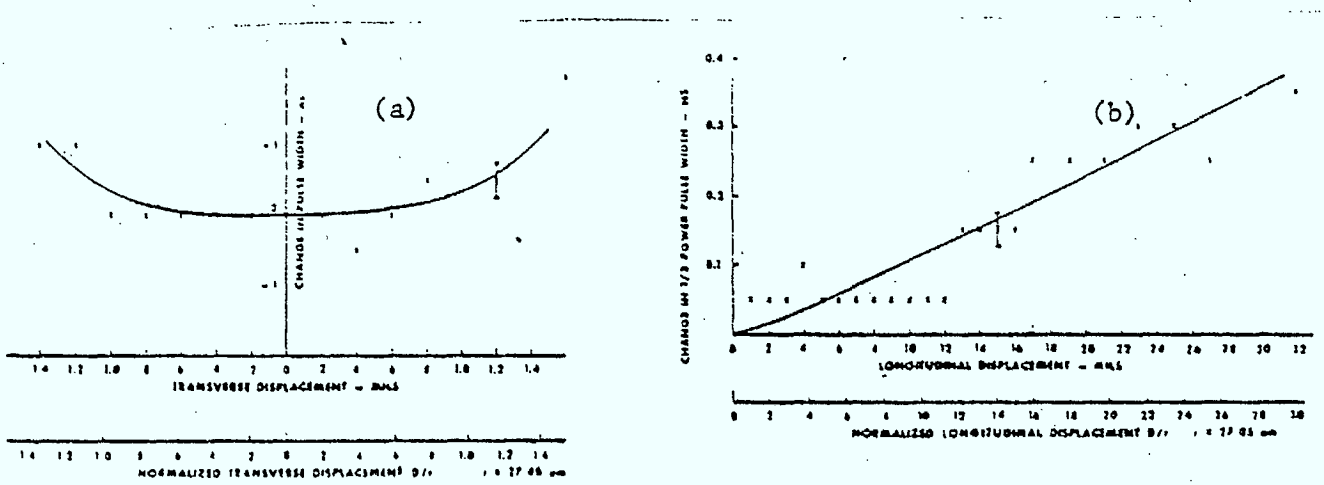

Figure 6.14: Same as Fig. 6.13 With Fiber Order Reversed.

presence of heavy mode mixing in the output fiber would tend to make pulse broadening rather insensitive to the exact launch conditions from the input fiber. This was confirmed when the experiments of Figure 6.13 were repeated with the normally lightly mixed output fiber now subjected to microbending via tension winding on a drum; the pulse broadening changed very little.

The importance of splices in a concatenated link was further emphasized in an installation of the British Post Office [112] using CGW fiber in BICC cable. Figure 6.15 shows an plot of multimode bandwidth (material dispersion removed) vs. concatenated length along one route. At three lengths (2,4, and 7 km) the bandwidth was higher than at the end of the previous section. This resulted from arranging fibers with alternately overcompensated and undercompensated profiles. Compensation refers to the degree by which higher order mode delays are reduced relative to lower order delays. (It can be probed by differential mode delay measurements or else by careful refractive index profile measurements.) Such an arrangement leads to some degree of optical multipath equalization along the route.

Recently, an investigation was made of several fiber types that had been characterized with respect to differential mode delay [131], and then concatenated (via a loose-tube splice) in pairs. The measurements were then repeated on the pairs from both ends. With high mode mixed fibers A, B (having an excess loss of 1 dB/km due to the fiber coating) the differential delay of A to B or B to A is controlled largely by the first fiber, A or B respectively; see Figure 6.16a. Figure 6.16b shows the results for low mixing fibers E, F; behaviour is reciprocal and equal to the simple sum of the individual delays. Note that at radial positions where the fibers have delays of opposite sign, some equalization is measured for the concatenation.

6.2.2.3 Wavelength Dependency of Equalization

The wavelength dependence of compensation effects [132] is shown in Figure 6.17. Measurements of bandwidth vs. wavelength showed that two fibers were each optimal near 750 and 1050 nm. The curve of the jointed pair is

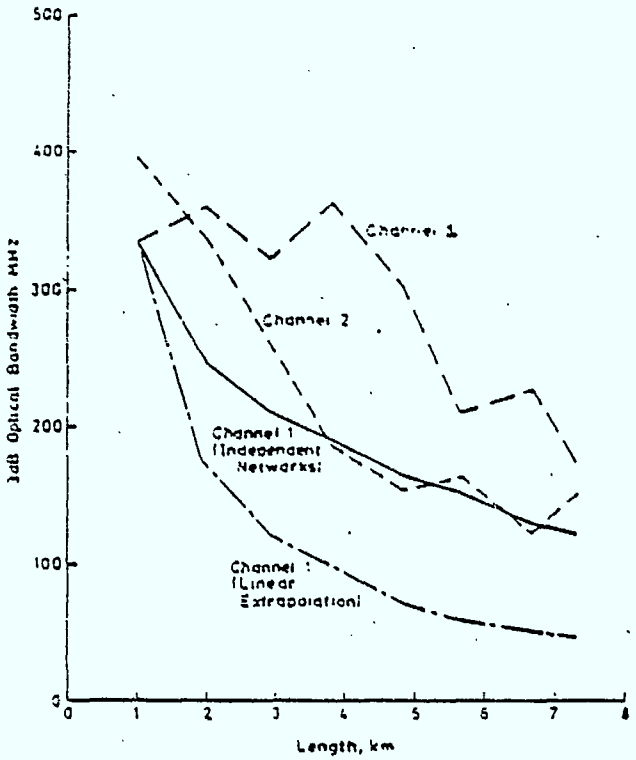

Figure 6.15
Bandwidth Versus Length, Showing Equalization Effects due to Opposite Compensations.

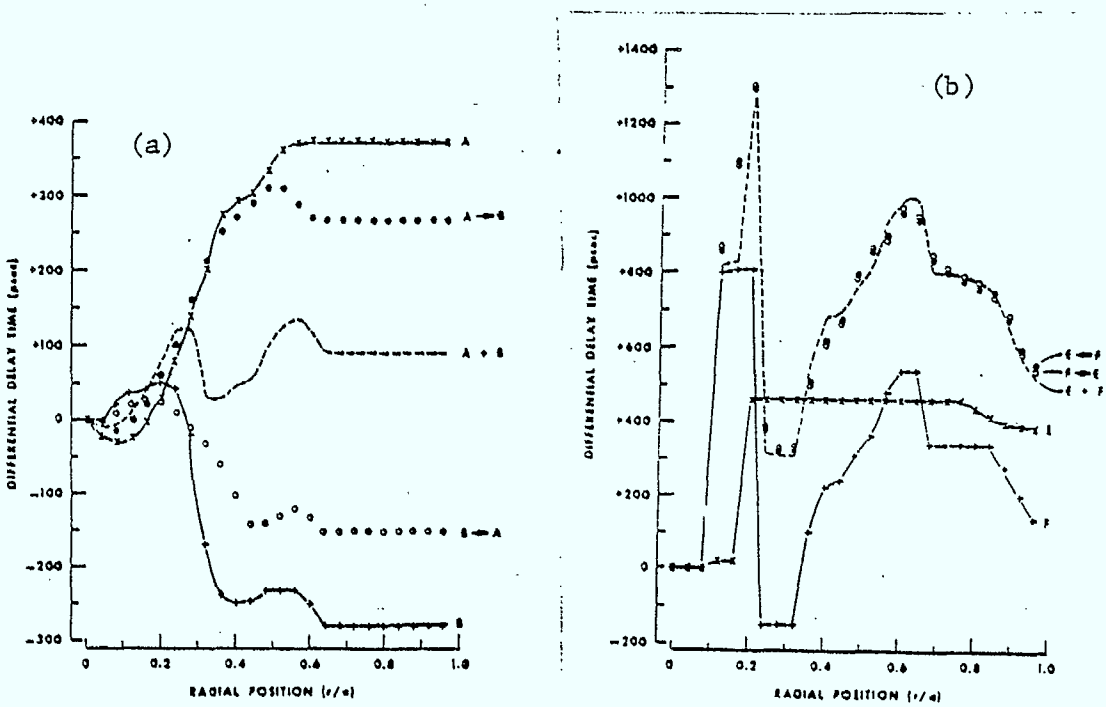

Figure 6.16: Differential Mode Delays of Individual and Concatenated Fibers in Both Directions: Heavy (a) and Light (b) Mode Mixing.

also seen wherein the two curves 'sum' to yield a stabilized variation of bandwidth vs. wavelength, although at a considerably reduced overall bandwidth. Note that due to profile dispersion, a fiber has opposite compensations at wavelengths on either side of its bandwidth peak. This was verified when another two fibers were jointed and the correlation coefficient was measured for three wavelengths; (λ, R) = (647 nm, +0.49), (835 nm, -0.26), (902 nm, +0.33). Compensations were the same sign at 647 nm, while at 835 nm one had switched. The second had switched between 835 and 902 nm. These results point out the fact that in a concatenated link the wavelength dependence of multimode dispersion arises from both fiber and joint properties.

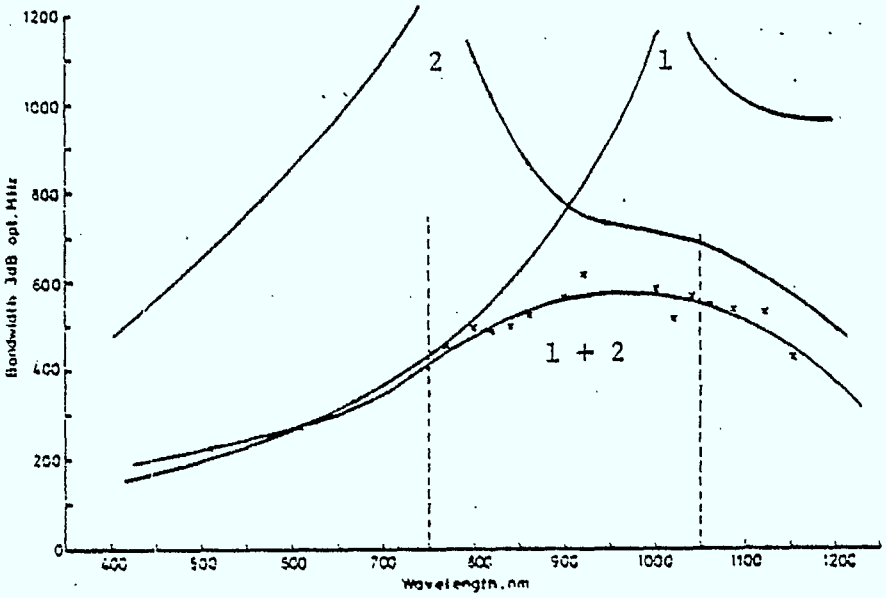

Figure 6.17
Bandwidth Versus Wavelength
For Two Fibers,
Before and After Jointing.

In a similar study [133], two fibers 2.3 and 2.4 km long had maximum bandwidths of about 800 MHz near 600 and 950 nm respectively. After fusion splicing, the 4.7 km length exhibited a 400 MHz bandwidth near 700 nm; these results are consistent with those of the previous paragraph. Moreover, both fibers were displaced up to 20 μm at the splice point. (This was apparently done prior to fusion). At 680 nm the bandwidth fell from 400 to 240 MHz whereas at 1060 nm it increased slightly from 170 to 180 MHz. These results were analyzed theoretically using the dispersive Olshansky - Keck extension to the Gloge-Marcatili power profile theory,

and then adding the lengths. Even after the assumption of uniform mode excitation and loss with no mode mixing, correlation with experimental results was close and agreeing with changes of compensation with wavelength. Relative displacement affects mode excitation and here increased loss and dispersion. Agreement with experiment is poor here, presumably because of imperfect profile fit and ignorance of the exact nature of the mode mixing.

6.2.3 Chromatic Dispersion

The significance of chromatic dispersion beyond about 3 km in a 12 km link [134] was accounted for by adding multimode and chromatic dispersions in the frequency domain (in GHz) similar to addition in the time domain (in nsec):

$$F^{-2} = L^{0.6}/0.8 + (T_c \, \Delta\lambda L/0.44)^2. \qquad (6.5)$$

Here T_c is the chromatic dispersion coefficient in nsec/km-nm, 0.8 GHz is the 3 dB multimode bandwidth at 1 km, and 0.44, is the Gaussian conversion factor into frequency domain.

6.2.4 Fiber Link Models

A large number of theories exist for dispersion along homogeneous fibers (see Section 4.4). A few theories exist for joint losses (see Section 5.5), but little on joint-induced dispersion. Even fewer models treat concatenated links. Each is correlated with only a very limited body of experimental data. Many theories require measurements of a nature not presently performed routinely, so it is unclear which will be useful in the long term.

6.2.4.1 Correlation Approach

Both a linear and root sum-of-squares addition seriously underestimated the resulting bandwidth in the BPO installation of Section 6.2.2.1. In a theoretical approach [135] to the equalization problem, the pulse spreading

T_1 along fiber 1 is regarded as obtained from the statistical variance of the probability distribution of the photon flight times down the fiber. If fiber 2 is jointed to fiber 1, the flight times in 2 are not independent; the total flight times are subject to a variance T where

$$T^2 = T_1^2 + T_2^2 + 2\, T_1\, T_2\, R_{12} \qquad (6.6)$$

and R_{12} is a joint correlation coefficient between the flight times. It has been recognized [136] that the individual variances T_1, T_2 and the joint correlation R_{12} may themselves be subject to the statistical fluctuations due to light launching, fiber variability and fiber jointing. This could lead to the specification of pulse broadening (or bandwidth) and jointing in terms of a mean value with some variance; the correlated total broadening of Equation (6.6) would be similarly expressed.

Little correlation across the joint is expected ($R_{12} \cong 0$) if mode mixing is heavy either within the fibers or at the joint as due to misalignment or fiber mismatching. This correponds to Gaussian or independent networks' sum-of-squares, but with improving fiber and jointing technology one expects $R_{12} \to 1$.

Then with similar fiber compensations on both sides of the joint, R_{12} is positive. This combined with little mode mixing yields the linear addition rule

$$T_{max} = T_1 + T_2. \qquad (6.7)$$

However, with opposite fiber compensations and little mixing, one has the equalization result

$$T_{min} = \left| T_1 - T_2 \right| . \qquad (6.8))$$

The extension to more than two fibers gives

$$T^2 = \sum_n T_n^2 + 2 \sum_n \sum_m T_n T_m R_{nm} . \qquad (6.9)$$

Additionally, if mode mixing is strong enough so that interaction between joints is minimal, this simplifies to the nearest-neighbor interaction rule for N sections:

$$T^2 (N) = \sum_{n=1}^{N} T_n^2 + 2 \sum_{n=1}^{N-1} T_n T_{n+1} R_{n,n+1} \qquad (6.10)$$

The correlation coefficient R can be theoretically calculated [137] for a number of special cases.

The practical implementation of the above approach is clouded by the fact that fibers from a particular manufacturer tend to all have the same compensation. Making use of the benefits of equalization would require a dual inventory of undercompensated and overcompensated fibers. This represents an added complication to the fabrication process where minimum dispersion has proven to be an elusive goal by itself. Moreover, a few measurements at BNR and at BTL have led to correlation coefficients greater than unity. This may be due to the neglect of non nearest-neighbor interactions, for example, or the use of FWHM instead of RMS; it warrants further investigation.

Some Norwegian experiments over 12 km of 9 fibers [113] found that the linear exprapolation rule did not 'seriously' underestimate concatenated pulse broadening. The laser line source was imaged across the fiber core and no mode scrambler was used. With such low mode mixing, a correlation coefficient R near +1 is implied (contrasted with 0.5 at the BPO) and it was thought that the neglect of nearest-neighbor interactions was unjustified in this case. No straightforward method for evaluating non-adjoining correlation seems to exist. Nevertheless, a modified correlation coefficient $R_{n,n+1}$ for the nth splice can be obtained from Equation (6.10)

$$T^2(n+1) - T^2(n) = T^2_{n+1} + 2T_n T_{n+1} R_{n,n+1} \qquad (6.11)$$

The values R_1 through R_8 averaged 0.7; 0.3 was recorded at a high loss splice but there was no apparent decrease with increasing length. All fiber sections were found to be overcompensated.

6.2.4.2 Modal Approach

Fibers specifically optimized for the 1.27 μm region were studied both individually and in a 48 km link [138] (average loss 0.61 dB/km, 0.13 dB/splice, average bandwidth 1.22 GHz-km). With chromatic dispersion subtracted out, the multimode dispersion transfer function at modulation frequency f out of a fiber length L is by definition

$$H_L(f) = \sum_m^M P_{out}(m,f) \; / \; \sum_m^M P_{in}(m,f). \qquad (6.12)$$

The sum extends over the total number of modes M. The output power in mode m can be expressed in terms of the input as

$$P_{out}(m,f) = P_{in}(m,f) \exp(-2\pi i f \tau_m) \qquad (6.13)$$

where τ_m is the group delay of that mode at length L. Differential mode attenuation can also be allowed for. The delays are calculated from measurements of the refractive index profile; they could be measured directly instead. At the qth joint between fibers q,q+1, the power into the latter fiber is modelled as

$$P_i^{(q+1)}(m,f) = (1-r)\, P_{out}^{(q)}(m,f) + r g(m) \sum_m^M P_{out}^{(q)}(m,f). \qquad (6.14)$$

Here r is a mode conversion factor which best-fits to a uniform value of 0.6. The mode redistribution function g is taken to be half-Gaussian with a half-width equal to 0.55 M. Substitution of the above two equations into $H_L(f)$ along with the link enables the 3 dB width of $H_L(f)$ to be calculated. Good agreement with measurements is found.

A similar modal approach using a "scattering matrix" representation has been reported in [139,140]. Little depth and experimental verification is offered.

6.2.4.3 Empirical Approach

A 'new parameter' theory [141] was used to closely describe along two links consisting of 2 km sections to total lengths of 15 and 53 km (Figure 6.18). First, the wavelength variation of bandwidth for each fiber is written in terms of its maximum value B at the optimum wavelength λ_o:

$$B^{-2}(\lambda) = B_o^{-2} + K^2(\lambda-\lambda_o)^2. \qquad (6.15)$$

Over the link, the total bandwidth is divided into correlated and uncorrelated parts involving multimode and chromatic dispersion. Further assumptions are made regarding a Gaussian source spectrum, mode mixing at the joint, and a mode diffusion process along the fibers. Values of various parameters are obtained from a combination of measurement and best-fit approaches, but the reward for such elaborate modelling is close correspondence with experimental concatenation measurements.

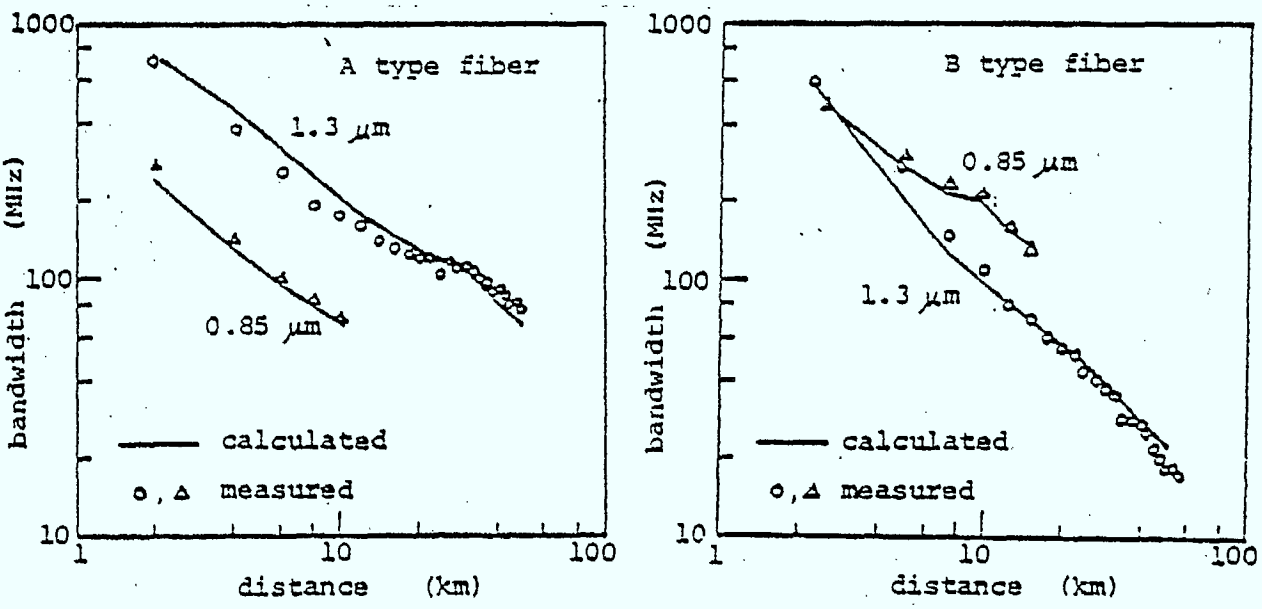

Figure 6.18: Bandwidth Versus Length For Two 53 km Links, Each Measured at Two Wavelengths, Compared With Theory.

6.2.4.3 Coupled Power Approach

We outline a final promising method [142] only qualitatively, since the equations and numerical methods involved are quite complex. The starting point is the time-dependent coupled-power equations for each fiber mode; they are written in terms of length and time derivatives of the modal pulse power $s_m(L,t)$. Parameters are the mode's group velocity, its attenuation coefficient, and its mode mixing parameter describing coupling to all other modes.

A Fourier transformation eliminates the time derivative and leaves a length derivative of the pulse spectrum $S_m(L,f)$. It is then recognized that S can be expanded in terms of central moments of s. These moments correspond to energy, mean delay, broadening, skewness, etc. and separate equations can be written for each of them. Closed-form solutions are possible for the two-mode case, and for a concatenated link three 'global' parameters arise: a coupling length, a pulse separation limit, and a splice mix factor, all of which can be defined mathematically. Some correspondence to the BPO correlation model is obtained, but further experimental input is required.

6.3 Discussion

The determination of the length evolution of attenuation of a concatenated link from the attenuation characteristics of individual fiber sections is complicated by the presence of joints and by the difference between the modal power distribution after each joint and in the measurement of individual fibers.

The length evolution of dispersion in a concatenated link has been characterized by empirical formulae. Their parameters are meant to lump together the effects of mode delay and mode mixing in the fibers and at the joints. These formulae are not adequate to predict bandwidth versus length because they include coefficients that, for now, can only be determined a posteriori (R_{nm}, Eqn (6.9)). Alternately, simple formulae like Equations (6.2) and (6.4) cannot reflect the non-monotonic evolution of bandwidth when over-and undercompensation alternates (Fig. 6.15).

A modal approach offers the promise of characterizing more completely and independently the various components of a fiber link. Consequently, this approach-while being more complex than simpler empirical formulae - should lead to a more general and more accurate line characterization.

7. PROPOSED WORK PROGRAM: THEORETICAL MODEL AND EXPERIMENTS

The above review of fiber system components has highlighted the dependence of their characterization on modal power distribution (MPD). Currently, many testing methods attempt to simulate an equilibrium or steady-state MPD. These methods ignore both the excitation dependence and length dependence of the components' behaviour. The steady-state attenuation or dispersion of a fiber is then independent of the type of source or joints in the upstream section.

In normal operation though, the system source launches into the fiber a MPD that differs usually from the steady-state condition. Similarily a joint tends to alter the steady-state MPD at the input of the downstream fiber.

Therefore, an operating system exhibits a two-fold behaviour: a steady-state and a transient behaviour. By definition the steady-state behaviour is a function of the fiber alone to the exclusion of any source or joint effects.

The transient behaviour characterizes both the fiber and the MPD at the source or at the joints. This behaviour is not unique to each fiber but will vary with the link configuration. The transient behaviour accounts for the difference between an actual system's performance and an all steady-state performance. This difference may be substantial. Both the magnitude of the transient behaviour and the length over which it exists are important to the system designer and to the evaluation of a working or faulty system.

Up until now, emphasis has been placed on steady-state characterization with very little attention for transient characterization. Testing methods suitable to the full characterization of a system and of its components need to be developed.

The work plan for this contract has two phases. Phase 1 calls for the development of a model for the various components of a fiber system. Phase 2 will use this model to simulate and compare various testing procedures. The model and its submodels will be developed during Phase 1 from a dual theoretical and experimental basis. During Phase 2 testing methods

will be implemented experimentally in accordance with the model and the conclusions of the simulations.

For completeness and for maximum flexibility the model will reflect the modal nature of propagation within a fiber system. The model will characterize modal attenuation, modal delay , mode mixing, spectral attenuation and chromatic dispersion. These characteristics will be represented in matrix format for fiber sections and for joints. Sources will be characterized by the power injected into various modes and represented in vector format. System performance will be obtained through recursive multiplication of appropriate matrices and vector.

The index profiles of actual fibers are not described exactly by an α-profile. Since minute deviations from the nominal α-profile reduce significantly the fiber bandwidth, it is essential to this activity that fibers of arbitrary profile be considered. Fibers will otherwise be assumed of circular symmetry. Inhomogeneity along the fiber axis will be modelled if necessary as a concatenation of shorter homogeneous but different sections.

The model will use the WKBJ quasi-ray theory of Sections 4.4.1 to account for the modal delay of fibers of arbitrary profile. An extension to arbitrary profile of the WKBJ approach of Section 5.5.1 will be used to represent mode mixing at the joints. Modal attenuation will be modelled according to Section 4.2.2 with the aid of experimental data. The experimental program will also measure the modal attenuation and delay of the fibers and the mode mixing in fibers and at the joints. Spectral delay and attenuation will also be incorporated.

Further work will be required to establish a theoretical link between modal power distribution and measurable characteristics like the near- or far-field patterns.

The above model is much more sophisticated and encompassing then the models reported in Sections 3 to 6. The reward for this increased level of complexity is the anticipation that it will lead to a faithful representation of a fiber link and to accurate predictions of system performance.

The above model will be used as a tool to research adequate testing methods. These methods will in turn lead to a complete appraisal of system performance as opposed to the restrictive and incomplete steady-state characterization of today's testing methods.

REFERENCES

[1] 'Multimode Optical Fibers: Steady State Mode Exciter', M. Ikeda et al, Appl. Opt. 15, 2116 (Sept. 1976)

[2] 'Transfer Function of Long Spliced Graded-Index Fibers with Mode Scrambler', M. Ikeda and K. Kitayama, Appl. Opt. 17, 63 (Jan. 1, 1978)

[3] 'Mode Scrambler for Optical Fibers', M. Ikeda et al, Appl. Opt. 16, 1045 (April 1977)

[4] 'Measurement of Loss and Output Numerical Aperture of Optical Fiber Splices' A.H. Cherin and P.J. Rich, Appl. Opt. 17, 642 (Feb. 15, 1978)

[5] 'Baseband-Frequence-Response Measurement of Graded-Index Fiber Using Step-Index Fiber as an Exciter', T. Tanifuji et al, Electron. Lett. 15, 203 (March 29, 1979)

[6] 'Far-End Measuring Methods for Transmission Characteristics of Graded Index Fiber', M. Tokuda et al, Proc. Int'l Conf. on Comm., Boston, paper 36.2 (June 1979)

[7] 'Measurement Method of Fiber Connection Loss Using Steady-State Power Distribution', Y. Daido et al, Top. Meet. Opt. Fib. Comm., Washington, Paper ThE3 (March 1979)

[8] 'Novel Mode Scrambler for Use in Optical Fiber Bandwidth Measurements', W.F. Love, Top. Meet. Opt. Fib. Comm., Washington, paper ThG2 (March 1979)

[9] 'Optical Loss Measurements in Graded-Index Fiber Using a Dummy Fiber', M. Tateda et al, Appl. Opt. 18, 3272-3275 (Oct. 1, 1979)

[10] 'Mode Conversion in Bent Step Index Multimode Fibers', M. Tateda and M. Ikeda, Appl. Opt. 15, 2308-2310 (October 1976)

[11] 'Measurement of Baseband Frequency Response of Multimode Fiber by Using a New Type of Mode Scrambler', M. Tokuda et al, Electr. Lett., 13, 146-147 (March 3, 1977)

[12] 'Effects of Different Mode Filters on Optical-Fiber Measurements', F.T. Stone and P.H. Krawarik, Top. Meet. Opt. Fib. Comm., Washington, paper ThG4 (March 1979)

[13] 'Mode Elimination in Fiber Loss Measurements', F.T. Stone and P.H. Krawarik, Appl. Opt. 18, 756 (March 15, 1979)

[14] 'Informal Contribution from Bell Tel. Lab. to Electr. Industries Assoc., Study Group P-6.6 on Optical Fibers and Materials (1979)

[15] 'A Fiber Concatenation Experiment Using a Standardized Loss Measurement Method', A.H. Cherin and E.D. Head, Symposium on Optical Fiber Measurements, Boulder, paper A.4 (Oct. 1980)

[16] 'Launching-Independent Measurements of Multimode Fibers', M. Eve et al, 2nd Europ. Conf. Opt. Fiber Comm., Paris, paper V.3 (Sept. 1976)

[17] CCITT Contribution COM XV, Philips (June 1979)

[18] 'Length-Dependent Attenuation Measurements in Graded-Index Fibers', R. Olshanksy et al, ibid [16], paper IV.5

[19] CCITT Contribution COM XV, - Nos. 58, ITT (August 1977); 64, Plessey and BICC (Sept. 1977); 65, UKPO (Sept. 1977); 72; Ericsson (Sept. 1977); 115, NTT (Jan. 1978); 153, Plessey (Jan. 1978)

[20] as above, 181, UKPO (May 1978)

[21] as above, Italy (June 1979)

[22] 'Comparative Measurements Regarding the Attenuation of Optical Fibers for the Eindhoven-Helmod Field Trial', A. Diekama et al, ibid [15], paper A.6

[23] 'An Accurate Method for the Measurement of Fiber Attenuations', A.B. Sharma et al, ibid [15] paper A.3

[24] "Propagation Parameter Measurements of Optical Waveguides", G.T. Holmes, Proc. SPIE, (April 1980)

[25] "Limited Phase Space Attenuation Measurements of Low-Loss Optical Waveguides", G.T. Holmes and R.M. Hawk, Opt. Lett. 6, 55 (Feb. 81)

[26] "Relations between Near-Field and Far-Field Intensities, Radiance, and Modal Power Distribution of Multimode Graded-Index Fibers", G. Grau and O. Leminger, Appl. Opt. 20, 457-459 (1 Feb. 1981)

[27] "Analytical Relations Between Modal Power Distribution and Near-Field Intensity in Graded-Index Fibers", S. Piazzola and G. De Marchis, Electr. Lett. 15, 721-722 (25th Oct. 1979)

[28] "Near-Field Intensity and Modal Power Distribution in Multimode Graded-Index Fibers", O. Leminger and G. Grau, Electr. Lett. 16, 678-679 (14 Aug. 1980)

[29] "Determination of Modal Power Distribution in Graded-Index Optical Waveguides from Near-Field Patterns and its Application to Differential Modal Attenuation Measurement", Y. Daido et al., Appl. Opt. 18, 2207-2213 (1 July 1979)

[30] "Measuring Fiber Connection Loss Using Steady-State Power Distribution: a Method", Y. Daido et al., Appl. Opt. 20, 451-456 (1 Feb 1981)

[31] "Observation of Tubular Modes in Multimode Graded-Index Optical Fibres", P. Faco et al, Electron. Lett. 16, 648 (Aug 1980), and references therein.

[32] "Selective Mode Excitation of Graded-Index Optical Fibers", L. Jeunhomme and J.P. Pocholle, Appl. Opt,. 17, 463 (1 Feb. 1978).

[33] "Differential Mode Attenuation Measurements in Graded-Index Fibers", R. Olshansky and S.M. Oaks, Appl. Opt. 17, 1830 (1 June 1978)

[34] "An Overview of Optical Time-Domain Reflectometry", M.D. Rourke, Physics of Fiber Optics, American Ceramic Society Annual Meeting, Chicago (April 1980)

[35] "Maximum Information Capacity of Fiber-Optic Waveguides", F.P. Kapron, Electr. Lett. 13, 96 (Feb. 1977)

[36] "Baseband Characteristics of Long-Wavelength LED Systems", D. Gloge et al, Electr. Lett. 16, 366 (May 1980)

[37] "Source and Modulation Effects in Monomode Fibers", F.P. Kapron, Sixth Europ. Conf. Opt. Comm., paper P3, York (Sept. 1980).

[38] "Material and Mode Dispersion in $GeO_2.B_2O_3.SiO_2$ Glasses"., J.W. Fleming, J. Am. Cer. Soc. 59, 503 (1976)

[39] "Interferometric Technique for the Determination of Dispersion in a Short Length of Single Mode Optical Fiber", W.D. Bomberger and J.J. Burke, Symp. on Opt. Fib. Meas. p. 101, Boulder (Oct 1980)

[40] "Experimental Method for the Separation of Material and Modal Dispersion of Optical Fibers", S. Seikai and K. Fussgaenger, ibid [37], paper P7

[41] "Optimization of Multimode Fiber Bandwidth via Differential Group Delay Analysis", M.J. Buckler and J.W. Shiever, ibid [37] paper 2.5

[42] "Cylindrical Dielectric Waveguide Modes", E. Snitzer, J. Opt. Soc. Am. 51, 491 (May 1961)

[43] "Fiber Optics .IX Waveguide Effects", N.S. Kapany and J.J. Burke, J. Opt. Soc. Am. 51, 1067 (Oct. 1961)

[44] "Optical Waveguide Theory", A.W. Snyder and J.D. Love, Chapman et al., London (1981)

[45] "Asymptotic Expressions for Eigenfunctions and Eigenvalues of a Dielectric or Optical Waveguide", A.W. Snyder, IEEE MTT-17, 1130 (Dec. 1969)

[46] "Weakly Guiding Fibers", D. Gloge, Appl. Opt. 10, 2252 (Oct 1971)

[47] "Dispersion in Weakly Guiding Fibers", D. Gloge, ibid [46], 2442 (Nov. 1971)

[48] "Leaky-Ray Theory of Optical Waveguides of Circular Cross Section", A.W. Snyder, Appl. Opt. 4, 273 (1974)

[49] "Length-Dependent Effects due to Leaky Modes on Multimode Graded-Index Optical Fibres", M.J. Adams et al., Optics Comm. 17, 204 (1976)

[50] "Solutions of Two Optical Problems", A. Fletcher et al, Proc. Roy. Soc. (London) 223, 216 (1954)

[51] "Modal Solution of a Point Source in a Strongly Focussing Medium", E.T. Kornhauser and A.D. Yaghjian, Rad. Sci. 2, 299 (Mar. 1967)

[52] "An Optical Waveguide with the Optimum Distribution of the Refractive Index with Reference to Waveform Distortion", S. Kawakami and J. Nishizawa, IEEE MTT-16, 814 (Oct. 1968)

[53] "Geometrical Optics of Parabolic Index-Gradient Cylindrical Lenses", F.P. Kapron, J. Opt. Soc. Am. 60, 1433 (Nov. 1970)

[54] "Scalar Analysis of Radially Imhomogeneous Guiding Media", W. Streifer and C.N. Kurtz, J. Opt. Soc. Am. 57, 779 (June 1967)

[55] "Time Dispersion in Dieletric Waveguides", S.D. Personick, Bell Syst. Tech. J. 50, 843 (1971)

[56] "Pulse Spreading Through a Dielectric Optical Waveguide", F.P. Kapron and D.B. Kirk, Appl. Opt. 10, 1519 (July 1971)

[57] "A Delay Formula for Arbitrary Ray Paths in Graded-Index Media", K.H. Steiner, NTZ 6, 250 (1974)

[58] "A Model for Ray Propagation in a Multimode Graded-Index Fiber", L. Jacomme, Opt. Comm. 14, 134 (May 1975)

[59] "Rays and Time Dispersion in Multimode Graded Core Fibers", M. Eve, Opt. Quant. Electr., 8, 285 (1976)

[60] "Pulse Dispersion in Optical Fibers of Arbitrary Refractive Index Profile", K.F. Barrel and C. Pask, Appl. Opt. 19, 1298 (April 1980)

[61] See the References in "Propagation Characteristics of Parabolic-Index Fiber Modes : Linearly Polarized Approximation", B.K. Garside et al, J. Opt. Soc. Am. 70, 395 (April 1980)

[62] "Modal Dispersion in Optical Fibers with Arbitrary Numerical Aperture and Profile Dispersion", E.A.J. Marcatili, Bell Syst. Tech. J. 56, 49 (1977)

[63] "Effects of Profile Deformations on Fiber Bandwidth", D. Marcuse and H.M. Presby, Appl. Opt. 18, 3758 (Nov 1979) and References Therein

[64] "Multiple - α Index Profiles", R. Olshansky, Appl. Opt. 18, 683 (March 1979)

[65] "Guided Waves in Inhomogeneous Focusing Media Part II: Asymptotic Solution for General Weak Inhomogeneity", C.N. Kurtz and W. Streifer, IEEE MTT-17, 250 (May 1969)

[66] "Effect of the Cladding on Pulse Broadening in Graded Index Optical Waveguide", R. Olshansky, Appl. Opt. 16, 2171 (Aug. 1977)

[67] "Profile Dispersion Characteristics in High-Bandwidth Graded-Index Optical Fibers", M. Horiguchi et al. Appl. Opt. 19, 3159 (Sept. 1980)

[68] "Propagation Characteristics of an Optical Waveguide with a Diffused Core Boundary", K.B. Chan et al, Electron. Lett. 6, 748 (Nov 1970)

[69] "Propagation of Electromagnetic Surface Waves in a Radially Inhomogeneous Optical Waveguide", J.G. Dil and H. Blok, Opto-Electronics 5, 415 (1973)

[70] "Comparison of Numerical Computations of Optical Waveguide Transmission Parameters", J.M. Arnold et al, Electron. Lett. 13, 273 (May 1977) and References Therein

[71] "Comparison of Calculated and Measured Impulse Responses of Optical Fibers", K. Okamoto, Appl. Opt. 18, 2199 (July 1979) and References Therein.

[72] "Pulse Dispersion in a Clad Lens-Like Medium", J. Rosenbaum and R. Cohen, Opt. Quant. Elect. 12, 109 (1980) and References Therein

[73] "Parabolic Fiber Cutoffs : A Comparison of Theories", T.I. Lukowski and F.P. Kapron, J. Opt. Soc. Am. 67, 1185 (Sept. 1977)

[74] "Propagation Constants and Group Delays of Guided Modes in Graded-Index Fibers : A Comparison of Three Theories", G. Jacobsen and J.J. Ramskov Hansen, Appl. Opt. 18, 2837 (Aug 1979)

[75] "Pulse Broadening in Multimode Optical Fibres with Large Δn/n : Numerical Results", J.A. Arnaud and J.W. Fleming, Electr. Lett. 12, 167 (April 1976) and References Therein

[76] "Mode Properties and Dispersion for Two Optical Fiber-Index Profiles by the Propagating Beam Method", M.D. Feit and J.A. Fleck, Jr., Appl. Opt. 19, 3140 (Sept 1980) and References Therein

[77] "Rigorous Evanescent Wave Theory for Guided Modes in Graded Index Optical fibers", J.M. Arnold and L.B. Felsen, IEEE MTT-28, 996 (Sept 1980) and References Therein

[78] "Evanescent - Wave and Non Linear Transformation Analysis of Graded-Index Fibers", G. Jacobsen, J. Opt. Soc. Am. 70, 1338 (Nov 1980) and References Therein

[79] "Numerical Calculation of Optimum α for a Germanium Doped Silica Lightguide", G.E. Peterson et al., Bell Syst. Tech. J. to be Published (March 1981)

[80] "Theory of Dielectric Optical Waveguides", D. Marcuse, Academic Press (1974)

[81] "Impulse Response of Clad Optical Multimode Fibers", D. Gloge, Bell Syst. Tech. J. 52, 801 (July-Aug, 1973) and References Therein

[82] "Numerical Solution of the Coupled-Power Equation in Step-Index Optical Fibers", M. Rousseau and L. Jeunhomme, IEEE MTT-25, 577 (July 1977)

[83] "Mode Coupling Coefficient Measurements in Optical Fibers", K. Kitayama and M. Ikeda, Appl. Opt. 17, 3979 (Dec. 1978)

[84] "Measurements of Mode Conversion Coefficients in Graded-Index Fibers", K. Nagano and S. Kawakami, Appl. Opt. 19, 2426 (July 1980)

[85] "Calculation of Bandwidth from Index Profiles of Optical Fibers. 1: Theory", D. Marcuse, Appl. Opt. 18, 2073 (15 June 1979)

[86] "Fusion Splicing of Optical Fibers", G.K. Pacey and J. Dalgleish, Electr. Lett. 15, 32-34 (4th Jan. 1979)

[87] "Splice Losses in Fusion-Spliced Optical Waveguide Fibers with Different Core Diameters and Numerical Apertures", D.R. Briggs and L.M. Jayne, Int. Wire and Cable Symposium, Cherry Hill, N.J., 356-361, (Nov. 1978)

[88] "The Effects on Joint Losses of Tolerances in Some Geometrical Parameters of Optical Fibers", D.J. Bond and P. Heusel, Opt. and Quant. Electr. 13, 11-18 (1981)

[89] "Fusion Splicing of Single-Mode Optical Fibers", M. Ogai et al, Proc. FOC' 80, 109-112 (1980)

[90] "Fusion Splices for Single-Mode Optical Fibers by Discharge Heating", I. Hatakeyanna and H. Tsuchiya, Trans. IECE of Jap. J62-C, 803-810 (1979)

[91] "Factors Affecting Performance of Optical Fiber Splices and Connectors", K.S. Gordon, Proc. FOC '80, 103-104 (1980)

[92] "Measuring Fiber Connection Loss Using Steady-State Power Distribution: a Method", Y. Daido et al., Appl. Opt. 20, 451-456 (1 Feb. 1981)

[93] "Field Measurement of Splice Loss Applying the Backscattering Method", P. Matthijsse and C.M. de Block, Electr. Lett. 15, 795-797 (22nd Nov. 1979)

[94] "Splice Loss Evaluation by Means of the Backscattering Technique", B. Costa et al., Electr. Lett. 15, 550 (30 Aug. 79)

[95] "Measurement of Optical Fiber Loss and Splice Loss by Backscatter Method", M. Nakahira et al., Trans. IECE of Jap. E-63, 762-767, (Oct. 1980)

[96] "Relation Between Splice Loss and Mode Conversion in a Graded-Index Optical Fiber", N. Kashida and N. Uchida, Elect. Lett. 15, 336-338 (7th June 1979)

[97] "Mode Conversion Properties of Different Splicing Techniques", M. Calzavara et al., 6th Europ. Conf. Opt. Comm., York, p. 318 (Sept. 1980)

[98] "Wavelength-Dependent Transmission at Fiber Connectors", K. Petermann, Electr. Lett. 15, 706-708 (25th Oct. 1979)

[99] "Splice Loss and Mode Conversion in a Multimode Fiber", N. Kashima, Appl. Opt. 19, 2597-2601 (1st Aug. 1980)

[100] "Characteristics of Optical Fiber Waveguides", R. Love and D. Keck, Opt. Eng. 17, 114 (March 78)

[101] "Transmission versus Transverse Offset for Parabolic - Profile Fiber Splices with Unequal Core Diameters", C.M. Miller, Bell Syst. Tech. J. 55, 917-927 (Sept. 1976)

[102] "A Loss Model for Parabolic - Profile Fiber Splices", C.M. Miller and S.C. Mettler, Bell Syst. Tech. J. 57, 3167-3180 (Nov. 1978)

[103] "A General Characterization of Splice Loss for Multimode Optical Fibers", Bell Syst. Tech. J. 58, 2163-2182 (Dec. 1979)

[104] "Contribution to Splice Loss Evaluation by the Backscatter Technique: A Statistical Comparison with Insertion Loss Data", A. Leboutet, Symposium on Fiber Measurements, Boulder, Co. (Oct. 1980)

[105] "Contributions of Optical-Waveguide Manufacturing Variations to Joint Loss", F.L. Thiel and D.H. Dairs, Electr. Lett. 12, 340 (24th June 1976).

[106] "Mode Conversion at Splices in Multimode Graded-Index Fibers", K. Kitayama, IEEE J. Quant. Electr. QE-16, 971-978 (Sept. 1980)

[107] "Reflection Losses from Imperfectly Broken Fiber Ends", D. Marcuse, Appl. Opt. 14, 3016-3020 (Dec. 1975)

[108] "Mode Conversion Caused by Splice of Graded-Index Fibers", Y. Daido et al., Trans. IECE of Jap. E-62, 363-367 (June 1979)

[109] "Pulse Distortion in Optical Fibers with Transverse Offset Splices", L. Bjerkam and H. Nordhy, Appl. Opt. 20, 435-439 (1 Feb. 81)

[110] "An Electromagnetic Analysis of the Transmission Properties of Radial Offsets in Round Optical Fibers", E. Bianciardi and V. Rizzoli, Digest Int. Microwave Symposium, IEEE MTT-S, 469-471 (1979)

[111] "Splice Loss Evaluation for Optical Fibers with Arbitrary-Index Profile", J. Sakai and T. Kimura, Appl. Opt. 17, 2848-2853 (1 Sept. 1978)

[112] "Transmission Studies on Three Graded-Index Fibre Cable Links Installed in Operational Ducts", M. Eve et al, Opt. Quant. Elect. 10, 253 (1978)

[113] "Comparison between Measured and Predicted Transmission Characteristics of 12 km Spliced Graded-Index Fibres", M. Eriksrud et al, Opt. Quant. Elect. 11, 517 (1979)

[114] "Measurements on Jointed Optical-Fibre Cables for the Slough-Maidenhead Field Trial", J.E. Taylor et al, IEE Proc. 127, 13 (Feb. 1980)

[115] "Propagation Parameter Measurements of Optical Waveguides", G.T. Holmes, Proc. SPIE, (April 1980)

[116] "Limited Phase Space Attenuation Measurements of Low-Loss Optical Waveguides", G.T. Holmes and R.M. Hawk, Opt. Lett. 6, 55 (Feb. 81)

[117] "Launch Dependent Attenuation Measurements on a 10-kilometer Concatenation Experiment", G.T. Holmes, 6th Europ. Conf. Opt. Fiber Comm., York, paper 6.2 (Sept. 1980)

[118] "The Length Dependence of Pulse Spreading in the CGW-Bell-10 Optical Fiber", E.L. Chinnock et al, Proc. IEEE, 61, 1499 (Oct. 1973)

[119] "First 560 Mb/s Trials on COS2 Optical Cable", A. Fansome and L. Sacchi, 2nd Europ. Conf. Opt. Fib. Comm., Paris, p. 564 (Sept. 1976)

[120] "Characteristics against Length of Silicone-Clad Silica Optical Fibers" I. Nouchi et al, Electr. Lett. 15, 315 (May 24, 1979)

[121] "Shuttle-Pulse Measurements of Pulse Spreading in an Optical Fiber", L.G. Cohen, Appl. Opt. 14, 1351 (June 1975)

[122] "Length Dependence of Pulse Dispersion in a Long Multimode Optical Fiber", L.G. Cohen and S.D. Personick, Appl. Opt. 14, 1357 (June 1975)

[123] "Shuttle Pulse Measurements of Pulse Spreading in a Low Loss Graded-Index Fiber", L.G. Cohen and H.M. Presby, Appl. Opt. 14, 1361 (June 1975)

[124] "Pulse Circulation Measurement of Transmission Characteristics in Long Optical Fibers", T. Tanifuji and M. Ikeda, Appl. Opt. 16, 2175 (Aug. 1977)

[125] "Measurement Methods of Optical Conductors' Transmission Characteristics", L. Jeunhomme et al, 2nd Europ. Conf. Opt. Comm., Paris, paper V.1 (Sept. 1976)

[126] "Dependence over 7 km of the Transfer Function of Graded Index Fibres", R. Bouillie et al, 2nd Europ. Conf. Opt. Comm., Paris,, Paper V.2, (Sept. 1976)

[127] "Transmission Characteristics of Mode Scrambler Loaded Long Length Spliced Graded Index Fibers", M. Ikeda and K. Kitayama, IOOC '77 Japan, Paper C3-4 (July 1977)

[128] "Characteristics of Graded-Index Fiber by VAD Method", S. Suzuki et al, 5th Europ. Conf. Opt. Comm., Amsterdam, Paper 12.6 (Sept. 1979)

[129] "Transmission Characteristics of 116.3 km and 65.1 km Graded-Index VAD Fibres at 1.55 μm and 1.3 μm", T. Edahiro et al, Electr. Lett. 16, 479 (June 5, 1980)

[130] "Delay Distortion Characteristics of Optical Fiber Splices", A.H. Cherin and P.J. Rich, Appl. Opt. 16, 497 (Feb. 1977)

[131] "Optimization of Concatenated Fiber Bandwidth Via Differential Mode Delay", M.J. Buckler, Symp. Opt. Fib. Measure., Boulder Co, paper C.3 (Oct. 1980)

[132] "Wavelength Dependence of Light Propagation in Long Fibre Links", M. Eve et al, 4th Europ. Conf. Opt. Comm., Genova, 58 (Sept. 1978)

[133] "Wavelength Dependence of Spliced Graded-Index Multimode Fibers", T. Matsumoto and K. Nakagawa, Appl. Opt. 18, 1449 (May 1, 1979)

[134] "100 Mb/s 12 km and 400 Mb/s 8 km Optical-Fibre Transmission Experiments", S. Sugimoto et al, Electr. Lett. 13, 637 (Oct. 13, 1977)

[135] "Statistical Model for the Prediction of the Bandwidth of an Optical Route", M. Eve, Electr. Lett. 13, 315 (May 26, 1977)

[136] "Bandwidth Characterization of Fiber Links", R. Iyer and A. Javed, 1980 IEEE/URSI Meeting, Quebec, Paper 7, Session C1/D (June 1980)

[137] "Multipath Time Dispersion Theory of an Optical Network", M. Eve, Opt. Quant. Electron. 10, 41 (1978)

[138] "Transmission Characteristics of Long Spliced Graded-Index Optical fibers at 1.27 μm", K. Kitayama et al, IEEE J. Quant. Electron. QE-15, 638 (July 1979)

[139] "Some Considerations of Transfer Function of Mode-Coupled Multimode Fiber", H. Kajioka, Trans. IECE of Jap., E-61, 749 (Sept. 78)

[140] "Transmission Theory of Mode-Coupled Multimode Fiber Based on Scattering Matrix", H. Kajioka, Trans. IECE of Jap. E-62, 546 (Aug. 79)

[141] "Estimation of Bandwidths of Long-Distance Graded-Index Fibers", T. Matsumoto, ibid [128], Paper 17.5

[142] "Pulse Broadening in Optical Fibers with Mode Mixing", S. Geckeler, Appl. Opt. 18, 2192 (July 1, 1979)

TESTING METHODOLOGIES FOR FIBER OPTIC TRANSMISSION SYSTEMS
v.1--Orientation report.